

# Quantum dynamics of the parabolic model

Pro Gradu  
Turun yliopisto  
Fysiikan ja tähtitieteen laitos  
Teoreettinen fysiikka  
2009  
LuK Jaakko Lehto  
Tarkastajat:  
  Dos. Pekka Lahti  
  Prof. Kalle-Antti Suominen

TURUN YLIOPISTO  
Fysiikan ja tähtitieteen laitos

**LEHTO, JAAKKO** Quantum dynamics of the parabolic model

Pro Gradu, 88 s.  
Teoreettinen fysiikka  
Marraskuu 2009

---

Kvanttimekaniikan teoriassa suljettuja, ympäristöstään eristettyjä systeemejä koskevat tulokset ovat hyvin tunnettuja. Eräs tärkeä erityispiirre tällaisille systeemeille on, että niiden aikakehitys on unitaarista. Oletus siitä, että systeemi on suljettu, on osaltaan tietysti vain yksinkertaistus. Käytännössä kaikki kvanttimekaaniset systeemit vuorovaikuttavat ympäristönsä kanssa ja tästä johtuen niiden dynamiikka monimutkaistuu oleellisesti. Kuitenkin tietyissä tapauksissa systeemin aikakehitys voidaan ratkaista, ainakin approksimatiivisesti.

Tärkeimpinä esimerkkeinä on ympäristön joko nopea tai erittäin hidas muutos kvanttisysteemin ominaiseen aikaskaalaan verrattuna. Näistä erityisesti jälkimmäinen on käyttökelpoinen oletus monissa fysikaalisissa tilanteissa. Tällöin voidaan suorittaa niin sanottu adiabaattinen approksimaatio. Sen mukaan systeemi, joka on aikakehityksen generoivan Hamiltonin operaattorin ominaistilassa, pysyy vastaavassa ominaistilassa ympäristön muuttuessa äärettömän hitaasti, mikäli systeemin eri energiatasot eivät leikkaa toisiaan. Todellisissa tilanteissa muutos ei tietenkään voi olla äärettömän hidasta ja myös energiatasojen leikkaukset ovat mahdollisia, jolloin tapahtuu transitio eri ominaistilojen välillä.

Energiatasojen leikkauksilla on oleellisia vaikutuksia erittäin monissa fysikaalisissa prosesseissa ja niitä kuvaamaan on luotu monia malleja kvanttimekaniikan alkua ajoista lähtien aina tähän päivään saakka. Nykyinen teknologinen kehitys on avannut uudenlaisen mahdollisuuden ilmiön kokeelliseen varmentamiseen ja hyödyntämiseen. Tämän vuoksi kyseisten mallien dynamiikan ja erityisesti energiatasojen useiden peräkkäisten leikkausten aiheuttamien koherenssi-ilmiöiden selvittäminen on tärkeää.

Tässä työssä käsitellään kvanttimekaanisia kaksitasosysteemejä, joissa esiintyy energiatasojen leikkauksia sekä niiden pitkän aikavälin dynamiikkaa. Tutkielmassa perehdytään tarkemmin kahteen tiettyyn malliin. Näistä ensimmäinen, Landau-Zener-malli, on tunnetuin ja sovelluksissa käytetyin malli. Kuitenkin erityisen mielenkiinnon kohteena on niin kutsuttu parabolinen malli, jolle johdetaan eri approksimaatioita käyttäen asymptoottiset transiitodennäköisyydet eri tilojen välille. Näitä verrataan numeerisiin tuloksiin.

Asiasanat: Kvanttidynamiikka, ei-adiabaattiset transiitot, parabolinen malli, Landau-Zener -malli, DDP-menetelmä, adiabaattinen approksimaatio.

# Contents

<b>Introduction</b>	<b>1</b>
<b>1 Introduction to two-level systems with time-dependent Hamiltonians and level crossings</b>	<b>5</b>
1.1 Basic formalism . . . . .	5
1.2 Adiabatic and diabatic approximations . . . . .	7
1.3 Level-crossing model . . . . .	11
1.4 Change of basis . . . . .	14
<b>2 The Landau-Zener model</b>	<b>19</b>
2.1 Differential equations . . . . .	19
2.2 Asymptotic expansions and the Stokes phenomenon . . . . .	21
2.3 Solution by Zener . . . . .	23
2.4 The S-matrix . . . . .	27
<b>3 Parabolic model</b>	<b>30</b>
3.1 The model . . . . .	30
<b>4 Approximative methods</b>	<b>35</b>
4.1 The independent crossing approximation . . . . .	36
4.2 Perturbation method . . . . .	38
4.3 DDP method . . . . .	40
4.3.1 Analytic behaviour of the eigenvalues . . . . .	41
4.3.2 Crossing point dominance . . . . .	45
4.3.3 Parabolic model in the DDP approximation . . . . .	53
4.4 The modified DDP method . . . . .	55
<b>5 Numerical studies</b>	<b>56</b>

<b>6</b>	<b>Results of Shimshoni and Gefen</b>	<b>60</b>
6.1	The independent crossing approximation . . . . .	61
6.2	A more general approximative solution . . . . .	65
<b>7</b>	<b>Comparison between different methods</b>	<b>69</b>
7.1	The double crossing case . . . . .	69
7.2	The tunneling case . . . . .	74
7.3	The phases in the independent crossing approximation . . . . .	74
<b>8</b>	<b>Conclusions</b>	<b>84</b>

## Introduction

Quantum mechanical level crossing problems have regained considerable attention in the recent years. Originally, the first level crossing model was introduced in the studies of inelastic atomic collisions as early as the 1930s [1, 2, 3]. Nowadays the topic is familiar in many different contexts in physics and with a wide variety of phenomena, for example in quantum information processing [4], laser-driven molecular wave packet dynamics [5], neutrino oscillations in astrophysics [6], tunneling between different energy bands of a semiconductor [7] or in mesoscopic superconducting circuits [8]. Clearly, the level crossing problems are not confined to any particular branch of physics. The reason is that the situation they cover is a quite generic one. When the discrete energy values of different states of a quantum mechanical system evolve in time, it might happen that these energy levels approach each other very closely or even cross at some points of time. There is a probability for the system to make a transition to another state because it becomes energetically possible at the vicinity of these points. The problem is then to find an expression for the transition probability between different states of the system.

The recovered interest in studying level crossing models is largely due to the fact that nowadays one is able to observe such genuinely time-dependent situations experimentally. One can modify the energy level structure of an atom for example by making it interact with an electromagnetic field and by those means induce time-dependent level crossings and couplings between the levels. This can be done for example with frequency-tunable lasers or placing the atom in a microwave cavity field or in a time-dependent magnetic field [9].

A two-level system is an elementary and basic framework for these kinds of studies, and indeed in this thesis, the level crossing models are considered in the two-level approximation. In quantum mechanics, a two-level system is a physical system which has a two-dimensional state space. There are many physical systems

which can be approximated by a two-level system. For example, systems in the low-temperature limit where only two of the energetically lowest-lying states are admissible and higher excitations can be neglected, or situations where we consider only the spin degree of freedom of a spin-1/2 particle. Even more importantly, at the viewpoint of this thesis, level crossings happen usually only with two levels at a time so near these degeneracy points the system can be considered as a two-level system.

Two-level systems are extremely important tool in quantum optics, being as simple as possible for studying transition dynamics but still providing some insight and methods for understanding more complicated systems. Their role is even more fundamental in the field of quantum information and quantum computation, constituting the physical implementation of qubits [10]. The great interest and development these research fields have gained in the past decades has made it also very important to be able to control the state of a two-level system interacting with its environment.

Although the rapid development of computers at the same time have made it possible to perform numerical simulations of quite complex quantum dynamics, the need for analytical methods and solvable models has not diminished because they are often much faster to solve at least in some parameter regions and they also offer better insight for example on the parameter dependence of the problem. Even within the two-level approximation, obtaining any analytic solution for the time evolution of a system is difficult and may usually be obtained only approximately. This leads to further approximations concerning the nature of the evolution.

For many physical systems, approximating the processes to be adiabatic is a natural choice. This can be done when the environment of a system is changing, in a sense, slowly enough. The adiabatic theorem ensures that in the limit of infinitely slow change, in a system initially prepared to an eigenstate of a time-dependent Hamiltonian there happens no transitions between the states and the state of the

system follows the instantaneous eigenstate that corresponds to the initial one. The adiabatic theorem is usually derived assuming the so-called "gap-condition" that the eigenvalue is separated from the rest of the spectrum. Of course in real physical systems the evolution is never strictly speaking infinitely slow and, as already mentioned earlier, energy level crossings are quite common, therefore breaking the validity of the adiabatic theorem so that there indeed are transition probabilities between the states. Such transitions that emerge from this breakdown are often called non-adiabatic ones.

Much of what is known about non-adiabatic transitions near the adiabatic limit can be summarized with a simple formula, a non-perturbative result first derived by Dykhne, stating that such transitions are exponentially suppressed [13, 14]. A mathematically rigorous proof of this result in the case of analytical Hamiltonian was later provided by Davis and Pechukas [15]. It is based on the analytic continuation of energy eigenvalues to the complex-valued time domain and integrating along a level line containing the complex crossing point nearest the real axis, that is, the complex plane zero point of the adiabatic energies which is shown to contribute most to the transition. Therefore we shall call their method of obtaining the final populations of the system as Dykhne-Davis-Pechukas method, abbreviated as DDP method. We shall discuss this important method in detail in chapter four of this thesis.

The first level crossing model was studied independently by Zener, Landau and Stückelberg in 1932. It consists of a two-level model where energy levels vary linearly in time having constant interaction between them. Nowadays it is known as the Landau-Zener model. It will be considered in chapter two and it serves as an introduction to crossing problems and to the methods for obtaining solutions to them. It is a very interesting and useful model also on its own because many more complicated crossing models can be reduced to it.

However, this is not always the case. There are situations where it is impossible to linearize the energy levels near the crossing point and to that end we consider a slightly more general setting where the linear time-dependence of energy levels is replaced by a parabolic one. We shall call this model as parabolic model or  $t^2$ -model and it too was first considered in collisional problems [31, 32, 33]. An interesting extra feature in this model is that now, depending on parameters, we have two crossings and the phase of the state becomes an observable. Therefore, it has raised interest also in the context of some interferometric schemes [29, 30].

The purpose of this thesis is to give an introduction to level crossing problems in the two-state approximation and in particular to the parabolic model. We consider different approximation methods and use them to solve the parabolic model in different parameter regions. We also discuss the difference between the results obtained in the references [28] and [41]. The model is solved also by performing numerical simulations and the approximative results are compared to these results.



# 1 Introduction to two-level systems with time-dependent Hamiltonians and level crossings

## 1.1 Basic formalism

We review some basic notions and definitions of the mathematical formulation of quantum mechanics and the problem at hand. In quantum mechanics, every physical system is associated with a Hilbert space  $\mathcal{H}$  and in the case of a two-level system this is a two-dimensional vector space over the complex numbers,  $\mathcal{H} = \mathbb{C}^2$ , so that every vector in it can be written as  $|\psi\rangle = (\psi_1, \psi_2)^T$  where  $\psi_i \in \mathbb{C}$ ,  $i = 1, 2$ . Elements of a Hilbert space are also called state vectors. In a Hilbert space, there is defined an inner product  $\langle \cdot | \cdot \rangle : \mathcal{H} \times \mathcal{H} \rightarrow \mathbb{C}$ . For  $\mathbb{C}^2$ , the inner product is just the familiar dot product  $\langle \psi | \varphi \rangle = \sum_{i=1}^2 \bar{\psi}_i \varphi_i$  for every  $|\psi\rangle, |\varphi\rangle \in \mathbb{C}^2$ , where the overhead bar stands for complex conjugation and the subscript indicates the component of a vector. If  $\langle \psi | \varphi \rangle = 0$  for two vectors  $|\psi\rangle, |\varphi\rangle \in \mathcal{H}$ , then those vectors are said to be orthogonal to each other. An inner product also defines a norm in the Hilbert space through  $\|\psi\| = \sqrt{\langle \psi | \psi \rangle}$  for all  $|\psi\rangle \in \mathcal{H}$ .

Every vector of norm one defines a one-dimensional projection  $\mathbf{P}[\psi]$  in  $\mathcal{H}$  with formula  $\mathbf{P}[\psi]|\varphi\rangle = (\langle \psi | \varphi \rangle) |\psi\rangle$ ,  $|\varphi\rangle \in \mathcal{H}$  and the elements of the set

$$\mathcal{P}(\mathcal{H}) = \{\mathbf{P}[\psi] \mid |\psi\rangle \in \mathcal{H}, \|\psi\| = 1\} \quad (1.1)$$

are called pure states. Any two pure states, say  $\mathbf{P}[\psi]$  and  $\mathbf{P}[\varphi]$ , can be combined into a new pure state  $\mathbf{P}[a\psi + b\varphi]$  with  $a, b \in \mathbb{C}$ , as long as  $a\psi + b\varphi \neq 0$  and normalisation of the vector is satisfied. This is called the principle of superposition. If a state is not pure it is called a mixed state. In any case, every state  $\rho$  of a quantum mechanical system can be given as a convex combination of pure states, which in the case of a two-level system means that an arbitrary state is of the form  $\rho = t_1\mathbf{P}[\psi_1] + t_2\mathbf{P}[\psi_2]$ ,  $0 \leq t_i \leq 1$ ,  $t_1 + t_2 = 1$ ,  $\mathbf{P}[\psi_i] \in \mathcal{P}(\mathcal{H})$ ,  $i = 1, 2$ . In this

thesis we consider only pure states. Clearly, from the axioms of the inner product, two vectors  $|\psi\rangle, |\varphi\rangle \in \mathcal{H}$  differing only by a phase factor  $e^{i\theta}$ ,  $\theta \in \mathbb{R}$ , define the same pure state. So, if  $|\psi\rangle = e^{i\theta}|\varphi\rangle$  then  $\mathbf{P}[\psi] = \mathbf{P}[\varphi]$  and there is a freedom of choosing the phase of a state vector. This does not mean that the phases of state vectors in different times are irrelevant. As it will be seen, in the context of the parabolic model, the superposition principle together with the phase differences give rise to observable interference effects.

Also worth mentioning is the usual Born rule that for a system in a some pure state  $\mathbf{P}[\psi]$ ,  $|\langle\varphi | \psi\rangle|^2$  is the probability to be in a state  $\mathbf{P}[\varphi]$  for all  $|\varphi\rangle \in \mathcal{H}$ . We introduce the quantity  $P$  which is the survival probability, and its counterpart, the overall transition probability  $Q = 1 - P$ .  $P$  is defined as

$$P = \lim_{t_0 \rightarrow -\infty} \lim_{t \rightarrow \infty} |\langle\psi(t) | \psi(t_0)\rangle|^2, \quad (1.2)$$

that is, the probability for the system to stay in the initial state  $\mathbf{P}[\psi(t_0)]$  when the system is first prepared in the infinite past and then it evolves to the infinite future. In this thesis we are interested in the asymptotic populations of two-level systems. We denote the probabilities for a system to be in states corresponding to levels one and two at a time  $t$ , respectively, by  $P_1(t)$  and  $P_2(t)$ . The asymptotic probabilities of the levels are written without explicit reference to time or to initial state as  $P_1$  and  $P_2$ .

We consider two-state systems with Hamiltonian operators that depend explicitly on time so that the time evolution of a state vector is given by the time-dependent Schrödinger equation:

$$i \frac{d}{dt} |\psi(t)\rangle = \mathbf{H}(t) |\psi(t)\rangle, \quad (1.3)$$

where  $\mathbf{H}(t)$  is the Hamiltonian that generates the time evolution. Here and throughout this thesis we have chosen  $\hbar = 1$ . Time-dependence of the Hamiltonian implies that the two-level system is not isolated from its surroundings but is, in fact, in an interaction with an environment. In principle, one could modify the description of

the physical system by including the environment to be part of it and that way end up with a time-independent Hamiltonian for this new enlarged system. In practise, for real systems the resulting mathematical model becomes too difficult. In any case, the solution to the Schrödinger equation (1.3) can be obtained by the unitary operator  $\mathbf{U}(t, t_0)$  that satisfies the relation  $|\psi(t)\rangle = \mathbf{U}(t, t_0)|\psi(t_0)\rangle$ , as the series [11]

$$\mathbf{U}(t, t_0) = \mathbf{I} + \sum_{n=1}^{\infty} (-i)^n \int_{t_0}^t dt_1 \int_{t_0}^{t_1} dt_2 \cdots \int_{t_0}^{t_{n-1}} dt_n \mathbf{H}(t_1) \mathbf{H}(t_2) \cdots \mathbf{H}(t_n). \quad (1.4)$$

## 1.2 Adiabatic and diabatic approximations

Assume that a system is coupled to an environment. When one wants to specify what is the effect on the state of the system when the environment is changing in a certain way, the result is known to depend largely on the length of the time interval on which the change is happening. The two limiting cases for the evolution, namely the diabatic and adiabatic approximations, are reviewed here shortly.

To do this, let  $T = t_1 - t_0$  be the time interval of the evolution on which the Hamiltonian is changing and replace the physical time by scaling  $s = (t - t_0)/T \in [0, 1]$ . Also it is convenient to denote the actual physical time evolution operator by  $\mathbf{U}(t, t_0) = \mathbf{U}_T(s)$ .

When the evolution is thought to be rapid, an approximation which shall here be called as the diabatic approximation is made. It is also commonly called sudden approximation in quantum mechanics but the reason for this kind of terminology used here is due to the mutual history and interference between collisional problems and level crossing studies. The connection shall be made clearer later. Now the change of the Hamiltonian takes place in a really short time interval and it can be thought to be instantaneous. When  $T$  tends to zero, the second term in the equation (1.4) vanishes and the time-evolution operator can be approximated as

$$\mathbf{U}_T(1) \simeq \mathbf{I}. \quad (1.5)$$

It should be noted that this is physically very intuitive. The evolution is so instantaneous and impulsive that the state of the system has not got time to react to this and change its functional form. Of course, this does not mean the same as that the system would not change at all. The eigenstates of the system change along with the Hamiltonian, and so do the eigenvalues as well, so a system that is initially in a stationary state does not usually remain in one.

This approximation is valid when [19]

$$T \ll \frac{1}{\Delta\bar{H}}, \quad (1.6)$$

where  $\Delta\bar{H}$  is the root mean square deviation for the initial state of the averaged Hamiltonian

$$\bar{H} = \frac{1}{T} \int_0^1 \mathbf{H}(s) ds. \quad (1.7)$$

In the opposite case, when the Hamiltonian is changing slowly, the adiabatic approximation can be used. The notion of adiabaticity has always played an important role in physics. Usually a physical process is considered to be adiabatic if it leaves invariant some essential property of the system involved in the process. In the case of quantum mechanics these are the stationary states. The adiabatic theorem of quantum mechanics concerns the long-time behaviour of a system, taking dynamical effects into account in the limit of slow change of the Hamiltonian which generates the evolution.

The idea of the adiabaticity in quantum mechanics was first formulated by Born and Fock in the late 1920s [16] but the modern formulation of the adiabatic theorem is due to T. Kato [17]. Although there are various versions of the problem and also generalisations to it, the traditional way to formulate the adiabatic theorem is to do it with the so-called "gap condition" [18]. It can be explained as follows.

The system is assumed to be initially in an instantaneous eigenstate of the Hamiltonian. It is then assumed that the corresponding eigenvalue is at all times isolated from the rest of the spectrum of the Hamiltonian, that is, there is a gap between

them. Now, in the limit of infinitely slow change, the state of the system stays at all times in the eigenspace corresponding to the initial one. This is formulated here explicitly in the case of a discrete Hamiltonian, so its spectrum consists entirely of its eigenvalues. Let  $s$ ,  $T$  and  $\mathbf{U}_T(s)$  be as defined before and let  $E_n(s)$ ,  $n = 1, 2, \dots$ , be the eigenvalues with the projections to respective eigenspaces denoted by  $\mathbf{P}_n(s)$ . It is assumed that all quantities involving the scaled time  $s$  are continuous and that the eigenvalues remain distinct at all times,  $E_m(s) \neq E_n(s)$  when  $m \neq n$ . Also it is assumed that  $\frac{d}{ds}\mathbf{P}_n(s)$  and  $\frac{d^2}{ds^2}\mathbf{P}_n(s)$  are well-defined and continuous. Now with these assumptions, let us state the adiabatic theorem: For all  $n = 1, 2, \dots$ , and  $|\psi\rangle \in \mathcal{H}$

$$\lim_{T \rightarrow \infty} \|\mathbf{U}_T(s)\mathbf{P}_n(0)|\psi\rangle - \mathbf{P}_n(s)\mathbf{U}_T(s)|\psi\rangle\| = 0. \quad (1.8)$$

A proof of the adiabatic theorem can be found for example in [19]. It can also be shown that for finite time intervals, the error term goes as  $\mathbf{O}(T^{-1})$  and depends on the time interval  $T$  and the size of the gap.

The existence of a gap is important because being able to give precise meaning to such terms as fast and slow change of a system, one has to have some intrinsic time scale in the system and the time scale is usually given by the gaps in the spectrum. Of course there might be some other property that gives the time scale. For example, even though the gap condition breaks down at the linearly crossing energy levels, there still is a characteristic time scale in the system given essentially by the inverse of the difference between the slopes of the eigenvalues [18].

Illustrating now the adiabatic approximation, consider a time-dependent Hamiltonian with a spectrum that is at every instant discrete and non-degenerate. Choose an orthonormal basis consisting of eigenstates  $|\phi_n(t)\rangle$  of the Hamiltonian  $\mathbf{H}(t)$  so that they are also time-dependent,

$$\mathbf{H}(t)|\phi_n(t)\rangle = E_n(t)|\phi_n(t)\rangle \quad (1.9)$$

and

$$\langle \phi_m(t) | \phi_n(t) \rangle = \delta_{nm}. \quad (1.10)$$

The state vector of the system at time  $t$  may be expanded in the orthonormal basis resulting

$$|\psi(t)\rangle = \sum_m c_m(t) \exp\left(-i \int_{t_0}^t E_m(t') dt'\right) |\phi_m(t)\rangle. \quad (1.11)$$

The exponent term in the middle is called the dynamical phase and the time-dependent Schrödinger equation (1.3) gives the equations for the expansion coefficients  $c_n(t)$  as

$$\begin{aligned} \dot{c}_n(t) = & -c_n(t) \langle \phi_n(t) | \dot{\phi}_n(t) \rangle \\ & - \sum_{m \neq n} c_m(t) \exp\left(-i \int_{t_0}^t (E_m(t') - E_n(t')) dt'\right) \langle \phi_n(t) | \dot{\phi}_m(t) \rangle, \end{aligned} \quad (1.12)$$

where the overhead dot stands for time derivation as usual. Differentiation of the equation (1.9) and multiplication by  $\langle \phi_m(t) |$  gives

$$\langle \phi_m(t) | \dot{\phi}_n(t) \rangle = \frac{1}{E_n - E_m} \langle \phi_m(t) | \dot{\mathbf{H}}(t) | \phi_n(t) \rangle, \quad m \neq n. \quad (1.13)$$

Now the evolution is considered adiabatic if

$$| \langle \phi_m(t) | \dot{\mathbf{H}}(t) | \phi_n(t) \rangle | \ll \frac{|E_n(t) - E_m(t)|}{\Delta T_{nm}}, \quad (1.14)$$

where  $\Delta T_{nm}$  is the characteristic time of transition between the states indexed with  $n$  and  $m$  which defines the time scale for the system. The characteristic time approaching to infinity is then obviously equivalent to that there are no transitions between the states and then also from the left side of the equation (1.14) it is seen that the matrix elements of the Hamiltonian change infinitely slowly. Then from the equation (1.13) it follows that

$$\langle \phi_m(t) | \dot{\phi}_n(t) \rangle \longrightarrow 0, \quad m \neq n. \quad (1.15)$$

The equation (1.12) for the coefficients then gives

$$\dot{c}_m(t) = -c_m \langle \phi_m(t) | \dot{\phi}_m(t) \rangle. \quad (1.16)$$

The initial condition that the state is initially in the  $n$ th eigenspace of the Hamiltonian can be expressed as  $c_m(0) = \delta_{nm}$  and in this case the adiabatic theorem follows:  $c_m(t) = 0$  for  $n \neq m$  and the equation (1.11) implies that

$$|\psi(t)\rangle = c_n(t) \exp\left(-i \int_{t_0}^t E_n(t') dt'\right) |\phi_n(t)\rangle. \quad (1.17)$$

Moreover, the coefficient  $c_n(t)$  can be calculated from equation (1.16). It is an additional phase factor

$$c_n(t) = e^{i\gamma(t)}, \quad (1.18)$$

where  $\gamma(t)$  satisfies the relation

$$\dot{\gamma}(t) = i\langle\phi_n(t) | \dot{\phi}_n(t)\rangle. \quad (1.19)$$

This extra phase factor is usually chosen to be equal to zero and a state vector satisfying the relation is said to be in the Born-Fock gauge [20]. However, this is not always possible and when the evolution is cyclic, this term gives rise to the Berry phase [36].

### 1.3 Level-crossing model

Instead of taking the environment of the two-level system explicitly into account it is assumed here that by considering the interactions or by some other means, one is able to write down the Hamiltonian for the two-level system alone. In this thesis we study cases where the Hamiltonian operator for a two-level system is represented as a real symmetric  $2 \times 2$  -matrix rather than as a complex Hermitian matrix. This is the case for systems with time-reversal symmetry [36]. The basic properties of such Hamiltonians are discussed next. So now we have

$$\mathbf{H}(t) = \begin{pmatrix} \beta_1(t) & V(t) \\ V(t) & \beta_2(t) \end{pmatrix}. \quad (1.20)$$

Here the real-valued functions  $\beta_1(t)$  and  $\beta_2(t)$  are the diabatic level energies and  $V(t)$  is the interaction term that couples the two levels with each other. Moreover,

we can also symmetrize the two diabatic energy levels by writing the state vector explicitly with a phase factor as

$$|\varphi(t)\rangle = \exp\left(-i \int^t \frac{\beta_1(\tau) + \beta_2(\tau)}{2} d\tau\right) \begin{pmatrix} C_1(t) \\ C_2(t) \end{pmatrix}, \quad (1.21)$$

where  $|\psi(t)\rangle = (C_1(t), C_2(t))^T$  is a vector satisfying the equation (1.3). Now, setting  $|\varphi(t)\rangle$  into that same equation, we end up with a convenient form of the time-dependent Schrödinger equation, the basic equation

$$i \begin{pmatrix} \dot{C}_1(t) \\ \dot{C}_2(t) \end{pmatrix} = \begin{pmatrix} \alpha(t) & V(t) \\ V(t) & -\alpha(t) \end{pmatrix} \begin{pmatrix} C_1(t) \\ C_2(t) \end{pmatrix}, \quad (1.22)$$

where it is defined  $\alpha(t) = (\beta_1(t) - \beta_2(t))/2$  and an overhead dot denotes the time derivative. Therefore there is no loss of generality in choosing the Hamiltonian to be traceless as well as real-symmetric.

The formula (1.22) is given in an orthonormal basis  $\mathcal{K}_d = \{|+\rangle, |-\rangle\}$  which we shall refer to as the diabatic basis and in which the basis vectors are written as

$$|+\rangle = \begin{pmatrix} 1 \\ 0 \end{pmatrix} \quad \text{and} \quad |-\rangle = \begin{pmatrix} 0 \\ 1 \end{pmatrix}. \quad (1.23)$$

When it is needed to emphasize the basis which is used, it is denoted as a subscript in the Hamiltonian,

$$\mathbf{H}_d(t) = \begin{pmatrix} \alpha(t) & V(t) \\ V(t) & -\alpha(t) \end{pmatrix}. \quad (1.24)$$

The eigenvalues of the Hamiltonian in (1.22), are obtained from the secular equation  $\det(\mathbf{H}(t) - \mathcal{E}_\pm(t)\mathbf{I}) = 0$  which gives

$$\mathcal{E}_\pm(t) = \pm\sqrt{\alpha(t)^2 + V(t)^2}. \quad (1.25)$$

Here  $\mathcal{E}_\pm(t)$  are the two possible outcomes for individual measurements of the system energy and they are called as the quasi-energies because the energy is not now conserved in the two-state system. They are also called the adiabatic energies because,



as it will be seen, they determine the adiabatic energy levels. The corresponding instantaneous normalised eigenvectors are

$$|\chi_1(t)\rangle = \mathcal{N} \begin{pmatrix} \frac{\alpha(t) + \sqrt{\alpha(t)^2 + V(t)^2}}{V(t)} \\ 1 \end{pmatrix} \quad \text{and} \quad |\chi_2(t)\rangle = \mathcal{N} \begin{pmatrix} \frac{\alpha(t) - \sqrt{\alpha(t)^2 + V(t)^2}}{V(t)} \\ 1 \end{pmatrix}, \quad (1.26)$$

where the normalisation factor  $\mathcal{N}$  is

$$\mathcal{N} = \frac{V(t)^2}{\mathcal{E}_\pm(t)^2 \mp \alpha(t)\mathcal{E}_\pm(t)}. \quad (1.27)$$

Depending on the functional form of the diabatic energy levels  $\alpha(t)$ , there may be such  $t_* \in \mathbb{R}$  that  $\alpha(t_*) = 0$  and  $\dot{\alpha}(t_*) \equiv \frac{\partial \alpha(t)}{\partial t}|_{t=t_*} \neq 0$  and if such points exist we say that we have an energy level crossing in those points. We call models with Hamiltonians having this property as level crossing models. In the case that the time-derivative of the diabatic energy levels would be zero at  $t_*$  the energy levels would only touch but not cross. If  $V(t_*) \neq 0$ , even when the diabatic energy levels cross each other the adiabatic energies usually merely approach each other but there is no real crossing. We shall call such situations as avoided crossings, often also called as pseudocrossings.

It is seen from the crossing model Hamiltonian written in (1.24) and from the discussion of the adiabaticity in the previous section, that there are two parameters which control the adiabaticity here. They are given by  $V(t_*)$  which is essentially the minimum distance between the different eigenvalues, in other words the size of the gap, and  $\dot{\alpha}(t_*)$  which corresponds to the rate of the change of the Hamiltonian at the time when the energy separation is smallest. So, roughly speaking, it can be concluded that when  $V(t_*) \gg 0$  and slowly-varying and  $\dot{\alpha}(t_*) \approx 0$  the adiabatic approximation applies. On the other hand, if  $V(t_*) \approx 0$  and  $\dot{\alpha}(t_*) \gg 0$  the evolution is best approximated diabatic. On the whole, it would be important to establish a theory which would give results in a similar manner for intermediate parameter values, interpolating between the two approximations.

## 1.4 Change of basis

As mentioned in the previous section, the framework for our studies was formulated in the diabatic basis. We could have chosen another basis for  $\mathbb{C}^2$  and it would have been an equally valid formulation of the physical problem. However, some basis may turn to be computationally more convenient than others, depending on the system and its parameters. We study here unitary transformations between different bases. Generally, a transformation  $\mathbf{U}$  is said to be unitary if its adjoint is equal to its inverse,  $\mathbf{U}^*\mathbf{U} = \mathbf{U}\mathbf{U}^* = \mathbf{I}$ . The unitary transformations leave the inner product invariant, that is, they map an orthonormal basis to another orthonormal basis.

It is a well known fact that the normalised eigenvectors of a self-adjoint operator form an orthonormal basis for  $\mathcal{H}$  in the finite-dimensional case. We call the basis formed from the instantaneous eigenstates of the diabatic Hamiltonian as the adiabatic basis and denote it as  $\mathcal{K}_a = \{|\chi_1\rangle, |\chi_2\rangle\}$ . When the Hamiltonian is time-dependent then also its eigenvalues are, and therefore also these basis vectors change with time, unlike the static diabatic basis vectors. Conversely we can also note that in the two-state case that is being studied, if there were no coupling between the two diabatic levels, then the diabatic basis vectors which are also orthonormal, would be the eigenvectors. Since we are interested here in the transition dynamics of the system, the non-diagonal terms are assumed to be non-zero and the bases are generally different.

On one hand, it may be suggested on the grounds of the adiabatic theorem that when the evolution of a system is nearly adiabatic and the system is initially in an eigenstate of the Hamiltonian, the state of the system follows closely the eigenstate and then using the adiabatic basis would be advantageous. On the other hand, if a system is changing rapidly, the state of the system has not got time to change its functional form and then formulating the problem in the time independent diabatic

basis is preferable. It can be shown that if

$$\lim_{t \rightarrow \pm\infty} |\alpha(t)| = \infty \quad \text{and/or} \quad \lim_{t \rightarrow \pm\infty} V(t) = 0, \quad (1.28)$$

then the energy levels of the different bases coincide when  $t \rightarrow \pm\infty$ , although depending on the model the level labels may be swapped [27]. Then the comparison between the results obtained in the different bases is straightforward because the initial and final probability distributions can be given in both bases simultaneously.

The relation between the two bases is now studied explicitly and the linear dependence between the adiabatic and diabatic basis vectors is established. In general, however, it should be noted when performing the two-state approximation, that it is possible that the two lowest adiabatic states would be combinations of more than just two diabatic states but it is clear from the introduction of the level-crossing model in the previous section that we do not consider such cases here.

At each instant  $t \in \mathbb{R}$ , we can diagonalize the Hamiltonian with a unitary transformation  $\mathbf{U}(t)$ , which is a  $2 \times 2$ -matrix that can be constructed by setting the instantaneous eigenvectors as its columns. Explicitly,

$$\mathbf{U}(t)\mathbf{H}(t)\mathbf{U}^*(t) = \mathbf{D}(t), \quad (1.29)$$

where  $\mathbf{D}(t) = \text{diag}(E_2(t), E_1(t))$  and  $\mathbf{U}(t) = (\chi_2^T(t) \mid \chi_1^T(t))$ . Now the change of basis from the diabatic basis to the corresponding adiabatic one is obtained through the relation

$$|\chi_{1,2}(t)\rangle = \mathbf{U}(t)|\pm\rangle. \quad (1.30)$$

When a vector  $|\psi(t)\rangle$  is transformed to another vector  $|\phi(t)\rangle = \mathbf{U}(t)|\psi(t)\rangle$  the time-dependent Schrödinger equation changes as

$$i \frac{d}{dt} [\mathbf{U}^*(t)\mathbf{U}(t)|\psi(t)\rangle] = \mathbf{H}(t)\mathbf{U}^*(t)\mathbf{U}(t)|\psi(t)\rangle \quad (1.31)$$

$$\Rightarrow i \frac{d\mathbf{U}^*(t)}{dt} |\phi(t)\rangle + i\mathbf{U}^*(t) \frac{d}{dt} |\phi(t)\rangle = \mathbf{H}(t)\mathbf{U}^*(t) |\phi(t)\rangle \quad (1.32)$$

$$\mathbf{U}(t) \cdot \Rightarrow i \frac{d}{dt} |\phi(t)\rangle = \left[ \mathbf{D}(t) - i\mathbf{U}(t) \frac{d\mathbf{U}^*(t)}{dt} \right] |\phi(t)\rangle. \quad (1.33)$$

So now, due to the time-dependence of the unitary transformations, the adiabatic Hamiltonian is not diagonal.

The usual and convenient way to write the transformation  $\mathbf{U}(t)$  is obtained by expressing the Hamiltonian in a different form [15],

$$\mathbf{H} = \begin{pmatrix} H_{11} & H_{12} \\ H_{21} & H_{22} \end{pmatrix} = \bar{E} \cdot \mathbf{I} + \frac{\delta E}{2} \begin{pmatrix} -\cos(\theta) & \sin(\theta) \\ \sin(\theta) & \cos(\theta) \end{pmatrix}, \quad (1.34)$$

where  $H_{12} = H_{21}$ ,  $\mathbf{I}$  is the identity matrix and the time-dependence of the elements is omitted for clarity. The quantities introduced in the previous formula are

$$\bar{E} = \frac{H_{11} + H_{22}}{2}, \quad (1.35)$$

$$\delta E = \sqrt{(H_{22} - H_{11})^2 + 4H_{12}^2}, \quad (1.36)$$

$$\tan(\theta) = \frac{2H_{12}}{H_{22} - H_{11}}, \text{ or equivalently} \quad (1.37)$$

$$e^{2i\theta} = \frac{H_{11} - H_{22} - 2iH_{12}}{H_{11} - H_{22} + 2iH_{12}}. \quad (1.38)$$

With these notations it follows easily that the eigenvalues of the Hamiltonian are  $E_1 = \bar{E} + \delta E/2$  and  $E_2 = \bar{E} - \delta E/2$  and the corresponding eigenvectors are

$$|\chi_1(\theta)\rangle = \pm \begin{pmatrix} \cos\left(\frac{\theta}{2}\right) \\ -\sin\left(\frac{\theta}{2}\right) \end{pmatrix} \quad \text{and} \quad |\chi_2(\theta)\rangle = \pm \begin{pmatrix} \sin\left(\frac{\theta}{2}\right) \\ \cos\left(\frac{\theta}{2}\right) \end{pmatrix}. \quad (1.39)$$

The eigenvectors are obviously orthonormal and real-valued for real  $t$  but determined only up to a factor of  $\pm 1$ .

Comparing the basis vectors between the adiabatic and diabatic bases as given in equations (1.23) and (1.39) it follows that the transformation between these bases is given by a matrix belonging to the representation of the  $SU(2)$  group which is also determined up to a sign and parametrized with  $\theta$ .

$$\mathbf{U}(t) = \pm \begin{pmatrix} \cos\left(\frac{\theta}{2}\right) & \sin\left(\frac{\theta}{2}\right) \\ -\sin\left(\frac{\theta}{2}\right) & \cos\left(\frac{\theta}{2}\right) \end{pmatrix}. \quad (1.40)$$

Applying these formulas explicitly to our real-symmetric and traceless Hamiltonian given in equation (1.24) we get  $\tan(\theta) = -\frac{V(t)}{\alpha(t)}$  and from equations (1.33) and (1.39) it is clear that the coupling between basis states exists even in the adiabatic basis, it has only changed its form:

$$\gamma(t) \equiv \langle \chi_1(t) | \dot{\chi}_2(t) \rangle \quad (1.41)$$

$$= \pm \frac{\dot{\theta}}{2} \quad (1.42)$$

$$= \pm \frac{V(t)\dot{\alpha}(t) - \alpha(t)\dot{V}(t)}{2(\alpha(t)^2 + V(t)^2)}. \quad (1.43)$$

This is the non-adiabatic coupling that follows from the explicit time-dependence of the Hamiltonian because it leads to the time-dependent unitary transformations between the bases.  $\gamma(t)$  vanishes at the adiabatic limit. Moreover, it depends on the relative sign of the adiabatic basis vectors given in (1.39). Now the Hamiltonian in the adiabatic basis is

$$\mathbf{H}_a(t) = \begin{pmatrix} -\mathcal{E}(t) & -i\gamma(t) \\ i\gamma(t) & \mathcal{E}(t) \end{pmatrix}, \quad (1.44)$$

where  $\mathcal{E}(t) = \sqrt{\alpha(t)^2 + V(t)^2}$  and  $E_i(t) = (-1)^i \mathcal{E}(t)$  are the adiabatic energy levels. Note that the adiabatic levels are chosen here in a such way that  $E_2(t) \geq E_1(t)$ .

A state vector in the adiabatic basis can be written as

$$|\Psi(t)\rangle = a_1(t)e^{-i\int_0^t E_1(s)ds}|\chi_1(t)\rangle + a_2(t)e^{-i\int_0^t E_2(s)ds}|\chi_2(t)\rangle, \quad (1.45)$$

where  $a_1(t)$  and  $a_2(t)$  are the probability amplitudes and exponential coefficients are the adiabatic dynamical phases. Inserting  $|\Psi(t)\rangle$  into the time-dependent Schrödinger equation, and operating left with  $e^{i\int_0^t E_k(s)ds}\langle\chi_k(t)|$ ,  $k = 1, 2$  we get the differential equations for the amplitudes  $a_k(t)$ ,  $k = 1, 2$

$$\dot{a}_1(t) = -\gamma(t)e^{-i\Delta(t)}a_2(t), \quad \dot{a}_2(t) = \gamma(t)e^{i\Delta(t)}a_1(t), \quad (1.46)$$

which follow from the orthogonality of the eigenvectors and the facts that

$\langle\chi_i(t)|\dot{\chi}_i(t)\rangle = 0$  and  $\langle\chi_2(t)|\dot{\chi}_1(t)\rangle = -\langle\chi_1(t)|\dot{\chi}_2(t)\rangle = -\gamma(t)$  and where it is

also defined

$$\Delta(t) = \int_0^t (E_2(s) - E_1(s)) ds. \quad (1.47)$$

Now the Schrödinger equation can be given in the adiabatic basis as

$$i \begin{pmatrix} \dot{a}_1(t) \\ \dot{a}_2(t) \end{pmatrix} = \begin{pmatrix} 0 & -i\gamma(t)e^{-i\Delta(t)} \\ i\gamma(t)e^{i\Delta(t)} & 0 \end{pmatrix} \begin{pmatrix} a_1(t) \\ a_2(t) \end{pmatrix}. \quad (1.48)$$

## 2 The Landau-Zener model

Probably the most familiar and also the simplest level crossing model is the Landau-Zener model, where the diabatic level energies vary linearly and the coupling between the levels is constant. It was first considered in papers published by Zener [1], Landau [2] and Stückelberg [3] as early as 1932. Although first used in inelastic atomic collisional problems, the Landau-Zener model has been used with a wide variety of physical phenomena over the years. The model has also been generalised to deal with more than just two energy levels [21]. The Landau-Zener model is defined by setting

$$\alpha(t) = \lambda t, \quad V(t) = V, \quad (2.1)$$

where  $\lambda$  and  $V$  are positive constants. Of course this simple model is not physically very realistic in the sense that the energy values are not bounded and the constant interaction between the levels lasts forever although the levels become more and more separated. Despite these shortcomings and its simplicity, the model has proven to be very important because usually when there is one or several isolated crossings, one is able to linearize the energy levels near them. One more important property of the model is that it can be solved analytically. Therefore it could also be used to study how well some of the approximate methods discussed later in this thesis will work.

### 2.1 Differential equations

The coupled first-order differential equations for the state vector elements resulting from the time-dependent Schrödinger equation (1.22) can be further differentiated to give two independent, second-order in time, differential equations

$$\ddot{C}_1 + (V^2 + \lambda^2 t^2 + i\lambda)C_1 = 0, \quad (2.2)$$

$$\ddot{C}_2 + (V^2 + \lambda^2 t^2 - i\lambda)C_2 = 0, \quad (2.3)$$

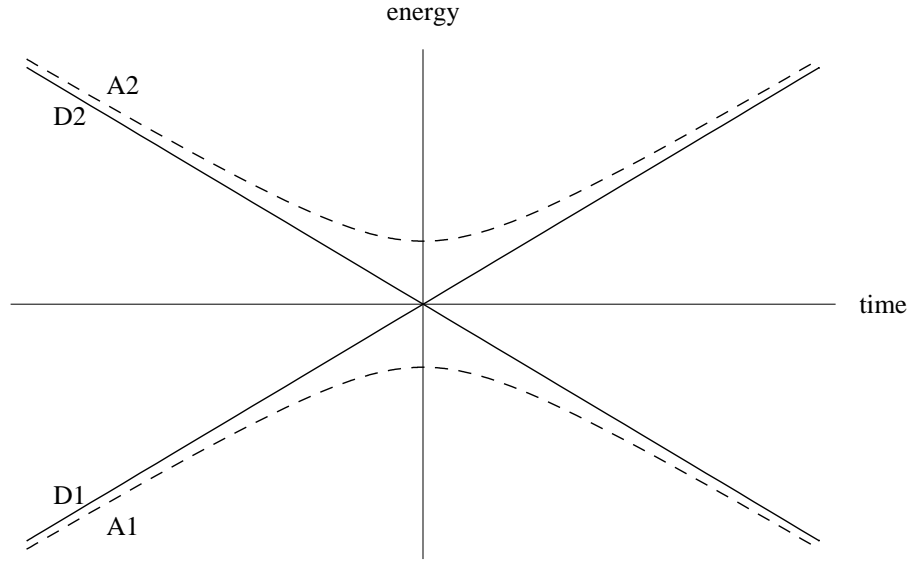


Figure 1. The time-dependence of the energy levels in the Landau-Zener model. The diabatic levels are drawn with solid lines and denoted with labels D1 and D2 while adiabatic ones are drawn with dashed lines and denoted with A1 and A2.

where the time dependence has not been explicitly written out. These equations can be cast into a solvable form by making a change of variables

$$z = \sqrt{2\lambda t} e^{-i\frac{\pi}{4}}. \quad (2.4)$$

Defining further

$$n = \frac{iV^2}{2\lambda} \equiv i\frac{\Lambda}{2} \quad (2.5)$$

and denoting with ( $'$ ) derivation respect to the new variable  $z$  we obtain the equations

$$C_2'' + \left( n + \frac{1}{2} - \frac{z^2}{4} \right) C_2 = 0, \quad (2.6)$$

$$C_1 - \frac{1}{V} \left( i\dot{C}_2 + \lambda t C_2 \right) = 0. \quad (2.7)$$

The positive parameter  $\Lambda = \frac{V^2}{\lambda}$  is related to adiabaticity of the system,  $\Lambda \rightarrow \infty$  being the adiabatic limit while  $\Lambda \rightarrow 0$  is the extreme non-adiabatic limit.

The differential equation for  $C_2$  has solutions in terms of parabolic cylinder functions  $D_n(z)$ , sometimes also called Weber functions. In turn, they can be written



with the help of confluent hypergeometric functions

$${}_1F_1(a, b; z) = 1 + \frac{az}{b} + \frac{a(a+1)z}{2!b(b+1)} + \frac{a(a+1)(a+2)z}{3!b(b+1)(b+2)} + \dots \quad (2.8)$$

as

$$D_n(z) = 2^{n/2} e^{-z^2/4} \left[ \frac{\sqrt{\pi}}{\Gamma(\frac{1-n}{2})} {}_1F_1\left(-\frac{n}{2}, \frac{1}{2}; \frac{z^2}{2}\right) - \frac{\sqrt{2\pi}z}{\Gamma(-\frac{n}{2})} {}_1F_1\left(\frac{1-n}{2}, \frac{3}{2}; \frac{z^2}{2}\right) \right]. \quad (2.9)$$

The description and numerous properties of the functions used here can be found for example in [22] and [23]. The differential equation (2.6) remains unaltered if the solution  $D_n(z)$  is replaced with  $D_n(-z)$ ,  $D_{-n-1}(iz)$  and  $D_{-n-1}(-iz)$ , so all these functions are also solutions. They are actually linearly independent solutions, so taking the initial conditions to be arbitrary, the general solution can be written as

$$C_2(z) = a_n D_n(z) + b_n D_n(-z), \quad (2.10)$$

where  $a_n, b_n \in \mathbb{C}$ .

## 2.2 Asymptotic expansions and the Stokes phenomenon

Being interested with the long-time behaviour of the solutions it is useful to study the asymptotic expansions of the parabolic cylinder functions when  $|z|$  is large. We say that two functions, say  $f(z)$  and  $g(z)$ , are asymptotic to each other as  $z$  tends to  $z_0$  if

$$\lim_{z \rightarrow z_0} \frac{f(z)}{g(z)} = 1. \quad (2.11)$$

Then the asymptotic relation is denoted as

$$f(z) \sim g(z), \quad z \rightarrow z_0. \quad (2.12)$$

Generalising the definition of the asymptotical equivalence in (2.11) to complex functions one must take into account that some paths in the complex plane may give nonunique limits. Therefore, the asymptotic expansion depends on the argument of

the complex variable  $z$  rather than being unique. The asymptotic expansions for parabolic cylinder functions with fixed  $n$ ,  $|z|$  is large and  $|z| \gg |n|$  are [23]

$$D_n(z) \sim e^{-z^2/4} z^n \left( 1 - \frac{n(n-1)}{2z^2} + \frac{n(n-1)(n-2)(n-3)}{2 \cdot 4z^4} - \dots \right), \quad (2.13)$$

$$\begin{aligned} D_n(z) \sim e^{-z^2/4} z^n \left( 1 - \frac{n(n-1)}{2z^2} + \frac{n(n-1)(n-2)(n-3)}{2 \cdot 4z^4} - \dots \right) \\ - \frac{\sqrt{2\pi}}{\Gamma(-n)} e^{n\pi i} e^{z^2/4} z^{-n-1} \left( 1 + \frac{(n+1)(n+2)}{2z^2} \right. \\ \left. + \frac{(n+1)(n+2)(n+3)(n+4)}{2 \cdot 4z^4} + \dots \right), \end{aligned} \quad (2.14)$$

$$\begin{aligned} D_n(z) \sim e^{-z^2/4} z^n \left( 1 - \frac{n(n-1)}{2z^2} + \frac{n(n-1)(n-2)(n-3)}{2 \cdot 4z^4} - \dots \right) \\ - \frac{\sqrt{2\pi}}{\Gamma(-n)} e^{-n\pi i} e^{z^2/4} z^{-n-1} \left( 1 + \frac{(n+1)(n+2)}{2z^2} \right. \\ \left. + \frac{(n+1)(n+2)(n+3)(n+4)}{2 \cdot 4z^4} + \dots \right), \end{aligned} \quad (2.15)$$

when  $|\arg(z)| < \frac{3\pi}{4}$ ,  $\frac{\pi}{4} < \arg(z) < \frac{5\pi}{4}$  and  $-\frac{5\pi}{4} < \arg(z) < -\frac{\pi}{4}$ , respectively.

Introducing the asymptotic expansions, the complex plane is now divided into different sectors by the domains of their validity in a such way that the limit (2.11) defining the asymptotic expansion is well defined on the sectors. Each sector has its own form of the asymptotic expansion of the function and the asymptotic expansion of the function is then a combination of these different terms. The term that is valid in a certain sector is said to be *dominant* in that sector while the other term is called *subdominant*, giving negligible contribution in the interior of that sector. Assume that  $f(z) \sim g(z)$  in some sector. We can write explicitly  $f(z) = g(z) + [f(z) - g(z)]$  and the second term is now just the subdominant one which can be neglected in the asymptotic relation. The edge of a sector is known as a *Stokes line*. When approaching this line, the subdominant term grows in magnitude comparable to the dominant part and can no longer be ignored. The leading behaviour of the asymptotic expansions becomes actually purely oscillatory at the Stokes line. Going over the Stokes line, the different terms in the asymptotic expansion swap their dominant and subdominant identities. This is known as *the Stokes phenomenon* [24].

The lines where the leading behaviour is purely real and therefore most unequal, exponentially increasing or decreasing, are called *anti-Stokes lines*.

The Stokes phenomenon is a purely mathematical concept but it is also physically relevant. The importance of the phenomenon can be illustrated with the help of the parabolic cylinder functions although the phenomenon is, of course, in no way confined to them. The Stokes phenomenon appears when there is an exponential function present in the asymptotic approximation [24]. From the equation (2.6) it is seen that the two controlling factors of the leading behaviour of the solution when  $|z|$  is large compared to  $n$  are  $e^{z^2/4}$  and  $e^{-z^2/4}$ . These functions are oscillatory when  $\arg(z) = \pm\pi/4$  or  $\arg(z) = \pm3\pi/4$ , defining the Stokes lines which in this case correspond to a  $\pi/4$ -rotation of the coordinate axes. Crossing these lines, the sign of  $\operatorname{Re}(\pm z^2/4)$  changes and the dominant and subdominant status of the terms is swapped. So now in our case, the increase in physical time  $t$  from the initial negative infinity corresponds to  $z$  approaching from the complex infinity to the origin on a Stokes line with angle  $3\pi/4$ , so that the second asymptotic expansion (2.14) is valid. Once it reaches the origin, the physical time becomes positive and now its increase corresponds to  $z$  receding from the origin on a line with  $\arg(z) = -\pi/4$ . Also at the origin, it crosses a Stokes line and the term that was earlier dominant becomes subdominant and the asymptotic expansion that is valid is now the equation (2.13). This is important because if the dominant part would be the same as initially then

$$\lim_{t \rightarrow -\infty} |C_i(t)| = \lim_{t \rightarrow \infty} |C_i(t)|, \quad (2.16)$$

and there would not be any transitions. Therefore, the existence of the Stokes lines can be seen as a condition for transitions to happen.

### 2.3 Solution by Zener

The results Clarence Zener originally obtained in [1] are reviewed here shortly. He considered a collision of two atoms with constant relative velocity and with an

assumption that the separation between the colliding partners is a known function of time. Moreover, he assumed that the transition region is so small that the energy separation of the two states is a linear function of time and the coupling between the levels could be regarded independent of time. This leads to (2.1) and of course to (2.6) and (2.7). Zener simplified the problem further by assuming the initial conditions

$$\begin{cases} |C_1(-\infty)| = 1, \\ C_2(-\infty) = 0, \end{cases}$$

where the rather obvious notation  $C_i(\pm\infty) = \lim_{t \rightarrow \pm\infty} C_i(t)$ ,  $i = 1, 2$ , is introduced. The same notation for the asymptotic amplitudes is also frequently used in what follows. The only solution satisfying these initial conditions is

$$C_2(z) = c_n D_{-n-1}(-iz), \quad (2.17)$$

where  $c_n \in \mathbb{C}$ . This is realised from the fact that  $D_n(y)$  vanishes for infinite  $y$  when  $\arg(y) < 3\pi/4$  by  $D_n(y) \sim \exp(-y^2/4)$  and from that  $\arg(-iz) = \pi/4$  is in the corresponding sector as  $t \rightarrow -\infty$ . The coefficient can be determined by putting (2.17) into (2.7) and using the initial condition for  $C_1$  ending up with equation

$$V = \lim_{t \rightarrow -\infty} |c_n \dot{D}_{-n-1}(-iz)|, \quad (2.18)$$

where it is possible to solve the modulus of the coefficient  $c_n$ . We choose to solve this a little bit differently.

$C_1(z)$  can be solved from the equation (2.7) and using the solution obtained for  $C_2(z)$ :

$$C_1(z) = \frac{1}{V} \left( i\dot{C}_2(t) + \lambda t C_2(t) \right) \quad (2.19)$$

$$= \frac{\sqrt{2\lambda}}{V} e^{i\frac{\pi}{4}} \left( C_2'(z) + \frac{z}{2} C_2(z) \right) \quad (2.20)$$

$$= \frac{\sqrt{2\lambda}}{V} e^{i\frac{\pi}{4}} c_n \left( D'_{-n-1}(-iz) + \frac{z}{2} D_{-n-1}(-iz) \right). \quad (2.21)$$

The diabatic energy levels cross at  $t = 0$ . We can calculate the amplitudes  $C_i(0)$ ,  $i = 1, 2$  as follows:

$$C_1(0) = \frac{\sqrt{2\lambda}}{V} e^{i\frac{\pi}{4}} c_n D'_{-n-1}(0), \quad (2.22)$$

$$C_2(0) = c_n D_{-n-1}(0). \quad (2.23)$$

Now,  $D_{-n-1}(0)$  and  $D'_{-n-1}(0)$  can be calculated by using the standard form of the solutions to the parabolic cylinder equation and the duplication formula for gamma function  $\Gamma(z)$  [22]

$$\Gamma(z)\Gamma\left(z + \frac{1}{2}\right) = 2^{1-2z} \sqrt{\pi} \Gamma(2z), \quad (2.24)$$

resulting in

$$D_{-n-1}(0) = -\sqrt{2} \frac{\Gamma(-n)}{\Gamma\left(\frac{1}{2} - \frac{n}{2}\right)} 2^{\frac{n}{2}} \sin\left(\frac{\pi n}{2}\right), \quad (2.25)$$

$$D'_{-n-1}(0) = 2i \frac{\Gamma(-n)}{\Gamma\left(-\frac{n}{2}\right)} 2^{\frac{n}{2}} \cos\left(\frac{\pi n}{2}\right). \quad (2.26)$$

By putting them back into equations (2.22) and (2.23) we can determine the absolute squares of the amplitudes. Since  $n$  is purely imaginary,  $\Gamma(n)^* = \Gamma(n^*) = \Gamma(-n)$  and by applying formulas [22]

$$\Gamma(n)\Gamma(-n) = -\frac{\pi}{n \sin(n\pi)}, \quad (2.27)$$

$$\Gamma\left(\frac{1}{2} - \frac{n}{2}\right) \Gamma\left(\frac{1}{2} + \frac{n}{2}\right) = \frac{\pi}{\cos\left(\frac{\pi n}{2}\right)}, \quad (2.28)$$

we find ( $n = \frac{i\Lambda}{2}$ )

$$|C_1(0)|^2 = \frac{2|c_n|^2}{\Lambda} \cosh\left(\frac{\Lambda\pi}{4}\right), \quad (2.29)$$

$$|C_2(0)|^2 = \frac{2|c_n|^2}{\Lambda} \sinh\left(\frac{\Lambda\pi}{4}\right). \quad (2.30)$$

Because these are probabilities they have to sum up to unity and the coefficient  $|c_n|$  is now easily found to be

$$|c_n| = \sqrt{\frac{\Lambda}{2}} e^{-\frac{\Lambda\pi}{8}}. \quad (2.31)$$

The probabilities at the crossing are now

$$P_1(0) = \frac{1}{2} \left( 1 + e^{-\frac{\Lambda\pi}{8}} \right), \quad (2.32)$$

$$P_2(0) = \frac{1}{2} \left( 1 - e^{-\frac{\Lambda\pi}{8}} \right). \quad (2.33)$$

The asymptotic probabilities  $P_1 = 1 - P_2$  are found by first using the identity

$$D'_{-n-1}(-iz) = iD_{-n}(-iz) - \frac{z}{2}D_{-n-1}(-iz) \quad (2.34)$$

to simplify the equation (2.21) into

$$C_1(z) = \frac{\sqrt{2\lambda}}{V} e^{i\frac{3\pi}{4}} c_n D_{-n}(-iz), \quad (2.35)$$

and then as  $t \rightarrow \infty$  we have  $-iz = re^{-i\frac{3\pi}{4}}$  with  $r \rightarrow \infty$  and we can use the asymptotic value (2.15)

$$D_{-n} \left( re^{-i\frac{3\pi}{4}} \right) \sim e^{-i\frac{r^2}{4}} \left( e^{-i\frac{3\pi}{4}} r \right)^{-n} - \frac{\sqrt{2\pi}}{\Gamma(n)} e^{i\frac{r^2}{4}} e^{i\frac{3\pi}{4}} \left( e^{i\frac{\pi}{4}} r \right)^n r^{-1}, \quad (2.36)$$

where only the first term remains and the value of  $P_1$  is found to be

$$\begin{aligned} P_1 &= \frac{2}{\Lambda} |c_n|^2 e^{-\frac{3\pi}{4}} \\ &= e^{-\pi\Lambda}, \end{aligned} \quad (2.37)$$

and for the other diabatic state

$$P_2 = 1 - e^{-\pi\Lambda}. \quad (2.38)$$

Initially, the system was in  $|+\rangle$  which coincides with  $|\chi_1(t)\rangle$  at the initial moment. In the adiabatic limit,  $\Lambda \rightarrow \infty$ , the final asymptotic populations are  $P_2 = 1$  and  $P_1 = 0$ . There is no contradiction because corresponding level labels between the diabatic and adiabatic levels are swapped at the crossing and  $|-\rangle$  coincides with  $|\chi_1(t)\rangle$  as  $t \rightarrow +\infty$ .

## 2.4 The S-matrix

In order to determine the asymptotic populations under general initial conditions, it is useful to introduce the  $S$ -matrix, the scattering matrix which maps the initial populations to the final ones. Because the total probability must be conserved the matrix is unitary. It is defined as

$$\begin{pmatrix} C_2(+\infty) \\ C_1(+\infty) \end{pmatrix} = \begin{pmatrix} S_1 & S_2 \\ -S_2^* & S_1^* \end{pmatrix} \begin{pmatrix} C_1(-\infty) \\ C_2(-\infty) \end{pmatrix}. \quad (2.39)$$

The  $S$ -matrix as defined is unitary when  $|S_1|^2 + |S_2|^2 = 1$ . It should be noted that the  $S$ -matrix maps the asymptotic populations according to their energies and in the Landau-Zener model the level with initially higher energy value becomes the lower one during the process, so the initial and final populations swap their places in the equation (2.39). The elements of the  $S$ -matrix are now calculated based on the exact solution (2.10). Calculations are similar to what is found in the reference [25].

As discussed, when  $t \rightarrow -\infty$  we have  $\arg(z) = 3\pi/4$  and  $\arg(-z) = -\pi/4$  so that their asymptotic expansions are (2.14) and (2.13), respectively. Using the general solution given in (2.10), the given asymptotic expansions and also making use of the polar form for the complex number  $z = re^{i\frac{3\pi}{4}}$ , we get

$$C_2(-\infty) = e^{-z^2/4} [a_n z^n + b_n (-z)^n] \quad (2.40)$$

$$= r^n e^{i\frac{r^2}{4}} e^{i\frac{3\pi n}{4}} [a_n + b_n e^{-i\pi n}] \quad (2.41)$$

$$= e^{i(\frac{3\pi n}{4} + \Phi)} [a_n + b_n e^{-i\pi n}], \quad (2.42)$$

where the last step is obtained using (2.4), where it follows that  $r^n = (2\lambda)^{\frac{n}{2}} |t|^n$  and defining  $\Phi$  as

$$\Phi \equiv \lim_{t \rightarrow -\infty} \left[ \ln(r^n e^{i\frac{r^2}{4}}) \right]. \quad (2.43)$$

It follows that this phase factor actually tends to infinity:

$$\Phi = \lim_{t \rightarrow -\infty} \left[ \frac{\lambda}{2} |t|^2 - i\frac{n}{2} \ln(2\lambda |t|^2) \right]. \quad (2.44)$$

The amplitude  $C_1(-\infty)$  is obtained in a similar fashion from the equation (2.7), using the identity [23]

$$D'_n(z) = nD_{n-1}(z) - \frac{z}{2}D_n(z), \quad (2.45)$$

to obtain the result

$$C_1(-\infty) = a_n \frac{2\sqrt{\pi\lambda}}{V\Gamma(-n)} e^{i(\frac{\pi n}{4} - \frac{3\pi}{4} - \Phi)}. \quad (2.46)$$

When  $t \rightarrow +\infty$  the arguments of the complex variables are swapped,  $arg(z) = -\pi/4$  and  $arg(z) = 3\pi/4$  and now we get

$$C_2(\infty) = e^{i(\frac{3\pi n}{4} + \Phi)} [a_n e^{-i\pi n} + b_n]. \quad (2.47)$$

This is all that is needed to determine the S-matrix of equation (2.39) because the previous formula for  $C_2(\infty)$  can be written in terms of the asymptotic initial populations. This is realised by defining

$$R = e^{-\frac{\pi\Lambda}{2}} \quad (2.48)$$

and

$$\chi = \frac{3\pi}{4} - arg \left[ \Gamma \left( i \frac{\Lambda}{2} \right) \right] + 2\Phi, \quad (2.49)$$

where the previously defined parameter  $\Lambda = V^2/\lambda$  is used and we can finally write

$$C_2(\infty) = \sqrt{1 - R^2} e^{i\chi} C_1(-\infty) + R C_2(-\infty), \quad (2.50)$$

from where the matrix elements  $S_1$  and  $S_2$  can be read out and then to obtain the other two elements is straightforward. Concluding,

$$\begin{cases} S_1 = \sqrt{1 - R^2} e^{i\chi} \\ S_2 = R \end{cases}. \quad (2.51)$$

It is easy to see that with the initial conditions (2.3), the result of Zener is obtained. Although Zener discussed his model in the context of a collisional process where the parameter controlling the energy level separation was the distance between colliding particles, a known function or equivalently a classical trajectory, he



neglected the fact that in a collisional process the crossing actually happens twice if the minimum distance in the process is smaller than the crossing distance. He therefore also neglected the coherence effects that result from this. A single crossing case happens only when the crossing distance is equal to a classical turning point of a collision and the validity of the model near the turning point is actually being questioned [26]. However, the Landau-Zener model has been proven to be a very successful one in practise.

### 3 Parabolic model

The usual procedure when two crossings are largely separated is to linearize the energy levels and treat the crossings as independent ones and then apply the Landau-Zener model twice. However, there are situations where the idea of separate level crossings does not work [28]. Next step after the linear model could be to consider models with parabolic time dependence of the energy levels and with constant coupling between them. We shall call this model as the parabolic model or  $t^2$  model. It can be used in a similar way to approximate more complex systems, covering also cases where the linearization fails, but it is a very interesting model also by itself.

Just like the Landau-Zener model, the parabolic model has been introduced in the context of slow atomic collisions [31, 32, 33] but can, of course, be used also in many other physical situations. The double crossing character mentioned already in the previous section is present in the parabolic model and it gives rise to interference effects due to the phase difference of the state vector that is accumulated between the crossings. Therefore it has also been studied in the context of molecular interferometry [29] and in a proposal of making a multiarm interferometer using a spinor Bose-Einstein condensate [30]. The analogy to quantum optical beam-splitter interferometers is clear, here the crossings just take the role of beam-splitters.

#### 3.1 The model

The parabolic model is defined as a model where the diabatic energy levels, instead of varying linearly in time as in the Landau-Zener model, are parabolic with respect to time. The coupling between the diabatic levels is still kept constant. This is done by setting the diabatic Hamiltonian matrix elements to be

$$\begin{cases} \alpha(t) = at^2 - b \\ V(t) = v \end{cases}, \quad (3.1)$$

where  $a$  and  $v$  positive parameters and  $b$  is a parameter which can be either positive, negative or zero. This leads to three different cases: if  $b > 0$ , we have a double crossing case for diabatic energy levels, a single crossing when  $b = 0$  and for values  $b < 0$ , there is no crossing and this is a tunnelling case. Naturally, also in the parabolic model, the adiabatic energy levels have avoided crossings in all those cases. The eigenvalues of the parabolic model Hamiltonian are

$$\mathcal{E}_{\pm}(t) = \pm \sqrt{(at^2 - b)^2 + v^2}. \quad (3.2)$$

The non-adiabatic coupling is now

$$\gamma(t) = \pm \frac{avt}{(at^2 - b)^2 + v^2}. \quad (3.3)$$

The coupling is antisymmetric with respect to time, that is  $\gamma(-t) = -\gamma(t)$ , and it is interesting to note that the magnitude of the non-adiabatic coupling has got two peaks regardless of  $b$ , that is, the double crossing character of the model does not vanish although the actual diabatic crossings do. These all are illustrated in the figure 2 for different cases.

The double crossing character can be understood by studying the adiabatic energy levels and their crossings. Although physically, that is when time is real, there are only two avoided crossings for the adiabatic energy levels, mathematically the equation  $\mathcal{E}(t) = 0$  of course has solutions when time  $t$  is taken to be a complex variable. Such points  $t_c \in \mathbb{C}$  are called complex crossing points. They will be discussed in detail in the context of the DDP method where they play a crucial role. For future purposes the complex crossing points for the parabolic model are given here by the equation

$$t_c = \pm \sqrt{\frac{b \pm iv}{a}}, \quad (3.4)$$

where one must take into account that  $b$  may be positive or negative. The complex crossing points are situated symmetrically with respect to the real and imaginary axes.

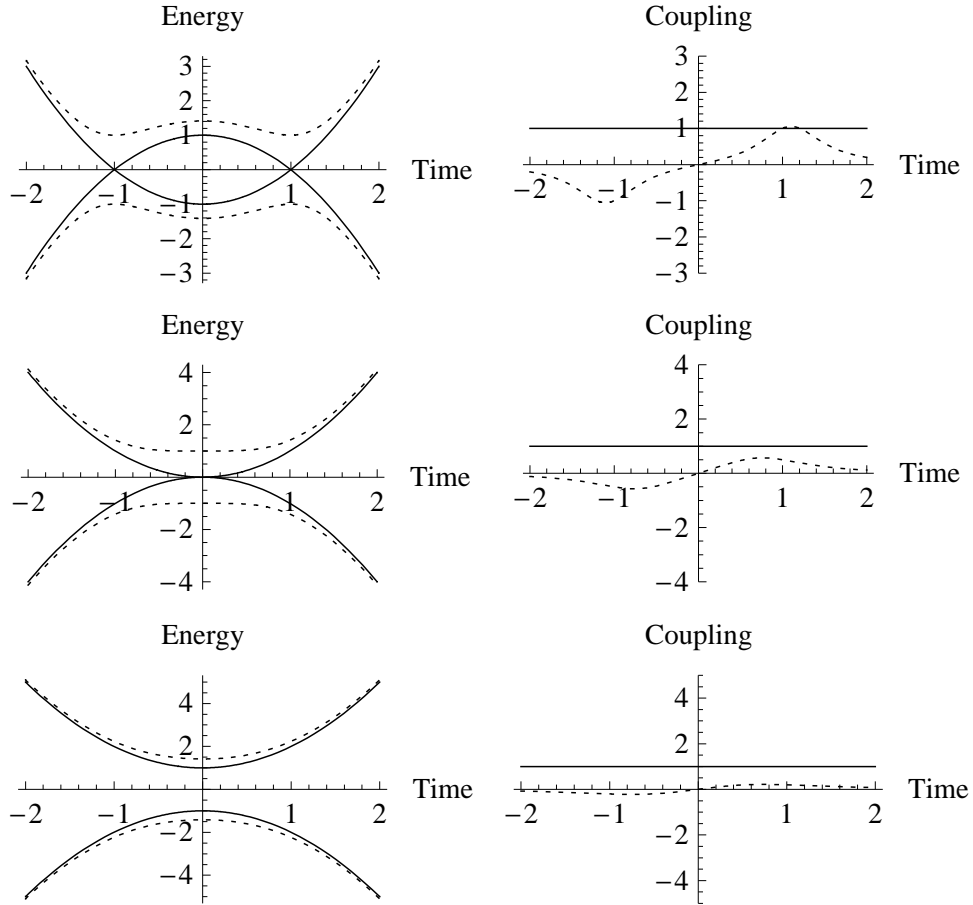


Figure 2. The three different cases in the parabolic model, from top to bottom:  $b > 0$ ,  $b = 0$ ,  $b < 0$ . On the left are the time dependencies of the energy levels and on the right are the corresponding level couplings. The diabatic quantities are marked with solid lines and the adiabatic quantities with dashed lines.

Also worth noticing is that when the time of the evolution is taken to be symmetric, the evolution for the parabolic model is actually cyclic in the sense that  $\mathbf{H}(+\infty) = \mathbf{H}(-\infty)$ . In the adiabatic limit, this would give rise to the Berry phase which for real-valued state vectors is just equal to  $\pm 1$  [36].

With three independent parameters, the adiabaticity parameter is not so evident. Also otherwise it is useful to use the scaling  $\tau = vt$  for time, so that the number of parameters reduces to two:  $\epsilon \equiv \frac{a}{v^3}$  and  $\mu \equiv \frac{b}{v}$ . This corresponds to setting the diabatic coupling equal to unity and just replacing the parameters  $a$  and  $b$  with  $\epsilon$  and  $\mu$ , respectively. This scaling is used in what follows. In the reference [28]

$\sqrt{\epsilon}$  is recognised as the adiabaticity parameter in the sense that  $\sqrt{\epsilon} \rightarrow 0$  is the adiabatic limit where the transition probability between the adiabatic states goes to zero. However, the situation here is also different from the Landau-Zener model because now the diabatic states do not swap their status during the evolution. This means that, for example, the diabatic state that corresponds to the lower adiabatic state initially corresponds to that also in the final time. Therefore, the behaviour is similar in both the large and small  $\sqrt{\epsilon}$  limit, that is, the transition probability for the diabatic states goes to zero in both limits as we shall see.

The diabatic energy levels cross the first time at  $\tau = -\sqrt{\mu/\epsilon} \equiv \tau_d^{(1)}$  and the second time at  $\tau = \sqrt{\mu/\epsilon} \equiv \tau_d^{(2)}$ , so the crossings are symmetrical with respect to the temporal zero point and the time interval between the crossings is  $\tau_s = 2\sqrt{\mu/\epsilon}$ . Assume that the system is initially in the lower basis state  $|- \rangle = |\chi_1(-\infty)\rangle$ . When one calculates the final state of the system in the parabolic model, that is, the asymptotic probabilities for the different basis states, it is seen that an interference effect is present. In certain parameter regions the transition probability depends sensitively on the parameters of the system. The interference emerges during the time interval between the crossings because the state of the system is then split into two partial waves which correspond to different "energy trajectories", as illustrated in the figure 3. The final state is then a superposition state of two partial waves which have traversed different paths between the crossings and their phases may therefore be different. The dynamical phase that is accumulated by the state vector of the system in the  $i$ th level with energy  $E_i$  during the time interval between  $\tau_0$  and  $\tau_1$  is

$$\phi_i = \int_{\tau_0}^{\tau_1} E_i(\tau') d\tau'. \quad (3.5)$$

It depends only on the energy and the time interval, so the dynamical phases that the two partial waves accumulate between the crossings are in general different. If the change of the phase between the crossings is large, the interference effects are

negligibly small when averaging over energy and instead of adding up the probability amplitudes to obtain the transition probability, the probabilities of the different versions of the transitions become additive [31].

In the diabatic basis the dynamical phase obtained by the level 1 during  $\tau_s$  is

$$\phi_1 = \int_{-\sqrt{\frac{\mu}{\epsilon}}}^{\sqrt{\frac{\mu}{\epsilon}}} (\epsilon x^2 - \mu) dx \quad (3.6)$$

$$= -\frac{4\mu^{3/2}}{3\sqrt{\epsilon}}, \quad (3.7)$$

and due to symmetry, for level 2 this is just  $\phi_2 = -\phi_1 \equiv \phi$  so that the phase difference accumulated is  $\sigma_d \equiv \phi_2 - \phi_1 = 2\phi = \frac{8\mu^{3/2}}{3\sqrt{\epsilon}}$ . For adiabatic states the difference of the dynamical phases acquired is now

$$\begin{aligned} \sigma_a &= 2 \int_{-\sqrt{\mu/\epsilon}}^{\sqrt{\mu/\epsilon}} \sqrt{(\epsilon x^2 - \mu)^2 + 1} dx. \\ &= \frac{2}{3} \sqrt{\frac{\mu}{\epsilon}} \left\{ 1 + 2 \sqrt{\frac{\mu+i}{\mu}} [\mu E(\varphi|k) - iF(\varphi|k)] \right\}, \end{aligned} \quad (3.8)$$

where  $F(\varphi|k)$  and  $E(\varphi|k)$  are the incomplete elliptic integrals of the first and second kind, respectively. They are defined as  $F(\varphi|k) = \int_0^\varphi d\theta / \sqrt{1 - k \sin^2(\theta)}$  and  $E(\varphi|k) = \int_0^\varphi d\theta \sqrt{1 - k \sin^2(\theta)}$  with the variables  $k = \arcsin\left(\sqrt{\frac{\mu}{\mu-i}}\right)$  and  $\varphi = \frac{\mu-i}{\mu+i}$ . When  $\mu$  gets large, which in our scaling corresponds to the case when separation of the diabatic energy levels near the temporal zero point is large compared to the coupling between the levels, the adiabatic phase difference tends to the same value as the diabatic case.

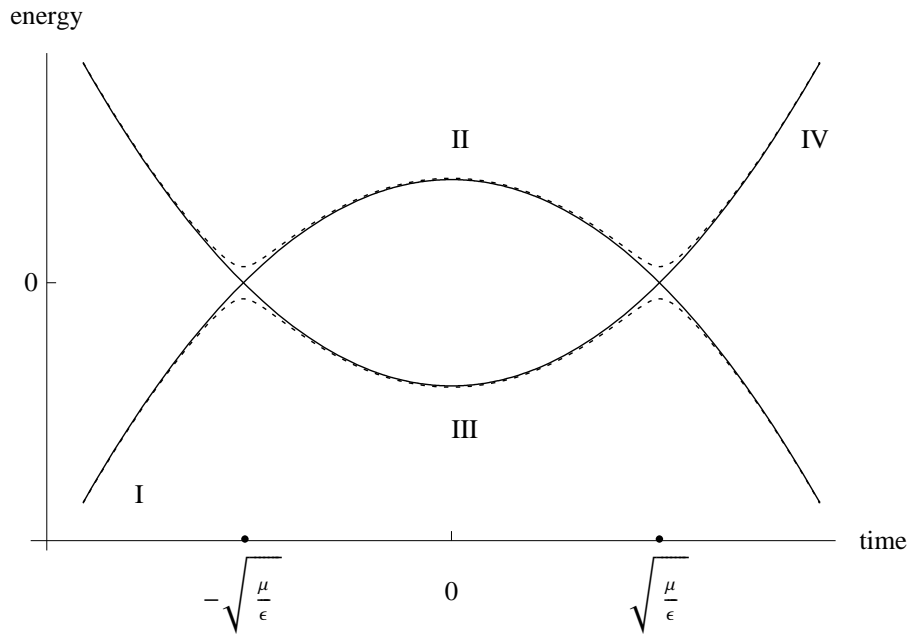


Figure 3. The two different trajectories, A and B, for a system initially in the low-energy level: A corresponds to the trajectory I-II-IV and B to I-III-IV. Diabatic levels are again drawn with solid line and the adiabatic levels are dashed.

## 4 Approximative methods

Unlike for the Landau-Zener model, the analytic solution for the parabolic model is not known. Therefore we are resorted to approximations and numerical methods. The rest of this thesis is devoted to these studies. Although with modern computers, the numerical simulations offer a strong alternative for more conventional analytic solution methods, even they become tediously hard in some parameter regions. The numerical method used is discussed in more detail in the next chapter.

The objective here is to find approximations that would cover the whole parameter range or at least a considerable amount of it so that one would get good approximations of the solutions fairly easily with all parameters. We consider four different approximation methods and their applicability, namely the perturbation series, the independent crossing approximation and the original and modified version of the DDP method. We find the quantity  $P_1 \equiv |C_1(\infty)| = |a_2(\infty)|$  in each of

the approximations with the initial conditions

$$|C_2(-\infty)| = |a_1(-\infty)| = 1, \quad C_1(-\infty) = a_2(-\infty) = 0, \quad (4.1)$$

and compare the results with the numerical ones in the next section.

#### 4.1 The independent crossing approximation

As discussed, many crossing models can be reduced to the Landau-Zener model. For parabolic model this is valid when the two crossings are so well separated that one can consider them as independent, hence the name for the approximation. The condition for this to be true is that the time interval between the two crossings,  $t_s$ , is considerably larger than the time scale of a single Landau-Zener transition denoted by  $t_z$ , which is for the limiting cases of adiabatic and diabatic approximations given by [34]

$$\begin{aligned} t_z &= \frac{V}{\lambda}, \quad \text{when } \Lambda \gg 1, \\ t_z &= \sqrt{\frac{\hbar}{\lambda}}, \quad \text{when } \Lambda \ll 1. \end{aligned} \quad (4.2)$$

The linearisation is done in the usual way by expanding the diabatic energy level into Taylor series at  $\tau = \tau_d = \pm\sqrt{\frac{\mu}{\epsilon}}$  and keeping the linear terms so that the truncated series forms a good approximation of the level near  $\tau_d$ . This gives

$$\alpha(\tau) \approx \alpha(\pm\tau_d) + \dot{\alpha}(\tau)|_{\tau=\pm\tau_d}(\tau \mp \tau_d) \quad (4.3)$$

$$= 2\sqrt{\epsilon\mu}\tau \mp 2\mu, \quad (4.4)$$

which gives an effective  $\lambda$ -term for the parabolic model,

$$\lambda_{\text{eff}} = 2\sqrt{\epsilon\mu}. \quad (4.5)$$

It follows that now the linearisation condition  $\tau_z \ll \tau_s$  would correspond to that in the adiabatic limit  $\frac{1}{4} \ll \mu$  would have to hold while in the diabatic limit the



condition requires that  $\mu^3/\epsilon \gg 1/256$ . If these do not hold, it means that the crossings overlap each other and they can not be considered as two separate events.

When calculating the asymptotic populations within the independent crossing approximation, the  $S$ -matrix of equation (2.39) is applied twice and the dynamical phase difference and the sign changes of the basis vectors must be taken into account:

$$|\psi(+\infty)\rangle = \mathbf{SAS}|\psi(-\infty)\rangle. \quad (4.6)$$

The matrix  $\mathbf{A}$ , which gives the change of the dynamical phases between the crossings, is different for different bases. It is given by

$$\mathbf{A} = \begin{pmatrix} e^{i\phi} & 0 \\ 0 & e^{-i\phi} \end{pmatrix}. \quad (4.7)$$

The  $S$ -matrices in the previous asymptotic formula are otherwise the same for both the adiabatic and diabatic basis as given by the equation (2.39) but the phase term obtained in the adiabatic basis is [9, 28, 32]

$$\chi = \frac{\pi}{4} + \frac{\Lambda}{2} \ln \left( \frac{\Lambda}{2e} \right) + \arg \left[ \Gamma \left( 1 - \frac{i\Lambda}{2} \right) \right]. \quad (4.8)$$

The phase term  $\chi$  is a monotonically decreasing function of  $\Lambda$  having the values between  $\pi/4$  and 0 and therefore being small in the adiabatic region of the parameter space.

The straightforward application of the equation (4.6) with initial conditions (4.1) gives the result of the independent crossings approximation as

$$P_1^{LZ} = 4e^{-\pi\Lambda_{\text{eff}}} (1 - e^{-\pi\Lambda_{\text{eff}}}) \sin^2(\chi + \sigma/2), \quad (4.9)$$

where it is defined similarly to the Landau-Zener model that  $\Lambda_{\text{eff}} \equiv \frac{V^2}{\lambda_{\text{eff}}} = \frac{1}{2\sqrt{\epsilon\mu}}$ . From the result (4.9) the interference effect is readily seen: there exists both an exponentially decaying part as well as a sine term which depends on the dynamical phases and the phase term  $\chi$ .

## 4.2 Perturbation method

The traditional way of solving problems approximately is to make use of perturbation theoretical methods in the weak coupling limit, where the general idea is that one obtains the solution for the real, more complicated, problem with the help of some simpler problem whose solutions are known. One considers a Hamiltonian for the real system which is written as the sum of the Hamiltonian for the simple unperturbed system and a relatively small perturbation term with some suitably chosen parameter which measures the strength of the perturbation. Then by continuity it is expected that one obtains the solution for the real problem as a series expansion in a such way that when the parameter vanishes, the real perturbed problem reduces to the unperturbed one and a good approximation would be obtained by considering a few first term of the series [35].

In quantum mechanics, Born approximation is most familiar in the context of scattering theory. Let  $\tilde{v}(\mathbf{r})$  be the interaction potential in the scattering process and  $\psi_0(t, \mathbf{r})$  be the state of the system in the absence of the interaction potential. Now the solution  $\psi(t, \mathbf{r})$  to the Schrödinger equation can be obtained formally as an integral equation:

$$\psi(t, \mathbf{r}) = \psi_0(t, \mathbf{r}) + \int G(t, \mathbf{r}, \mathbf{r}') \tilde{v}(\mathbf{r}', t') \psi(t', \mathbf{r}') d\mathbf{r}', \quad (4.10)$$

where  $G(t, \mathbf{r}, \mathbf{r}')$  is the propagator. Now  $\psi(t, \mathbf{r})$  is on both sides of the equation, but it can be solved iteratively. The result is a series called Born series and the (first) Born approximation consists of considering only the first term of the series [11, 35].

Of course in our case we study only the time-dependence of the system. By taking the coupling term to be a small perturbation we end up with a similar iterative integral equation scheme. In the adiabatic basis it follows from the initial conditions (4.1) and from the equation (1.48) that the Born approximation now

yields

$$|a_2(\infty)|^2 = \left| \int_{-\infty}^{\infty} \gamma(t) e^{i\Delta(t)} dt \right|^2. \quad (4.11)$$

Because the coupling is weak, it can not change the amplitudes substantially from the initial ones and we can take in the first Born approximation  $a_1(t) = 1$ . However, as indicated in [25, 27] the validity and usefulness of the Born approximation in adiabatic basis is questionable. In the diabatic basis it gives reasonably good results in a suitable parameter region as will be seen for the parabolic model.

Now in the diabatic basis when the diabatic coupling  $v$  is small we consider it to be a small perturbation for an unperturbed "free atom" whose energy levels are not coupled. In the scaling used, the relative smallness of the perturbation corresponds to  $\epsilon$  and  $\mu$  being large. In the diabatic basis, the Born approximation gives

$$P_1^{Born} \equiv \left| \int_{-\infty}^{\infty} V(\tau) \exp \left[ -2i \int^{\tau} \alpha(\tau') d\tau' \right] d\tau \right|^2 \quad (4.12)$$

$$= \left| \int_{-\infty}^{\infty} \exp \left[ -2i \int^{\tau} (\epsilon\tau'^2 - \mu) d\tau' \right] d\tau \right|^2 \quad (4.13)$$

$$= \left| \int_{-\infty}^{\infty} \cos \left( \frac{2\epsilon\tau^3}{3} - 2\mu\tau \right) d\tau \right|^2 \quad (4.14)$$

$$= \left| \frac{2\pi}{\sqrt[3]{2\epsilon}} Ai \left[ -\frac{2\mu}{\sqrt[3]{2\epsilon}} \right] \right|^2, \quad (4.15)$$

where the last steps follow by writing the exponent term as  $e^{ix} = \cos(x) + i \sin(x)$  and the sine function is odd so its integral vanishes. The integral that is then left is just the Airy function  $Ai[\cdot]$  [22]. The expression can be further simplified and approximated with large  $\mu$ ,

$$P_1^{Born} = \pi^2 \left( \frac{4}{\epsilon} \right)^{2/3} \left( Ai \left[ -\mu \left( \frac{4}{\epsilon} \right)^{1/3} \right] \right)^2 \quad (4.16)$$

$$\sim \frac{\pi}{\sqrt{2\epsilon|\mu|}} \exp \left[ -\frac{1}{3} \sqrt{\frac{8|\mu|^3}{\epsilon}} \right], \quad \mu < 0 \quad (4.17)$$

$$\sim \frac{2\pi}{\sqrt{\epsilon\mu}} \sin^2 \left( \sqrt{\frac{4\mu^3}{\epsilon}} + \frac{\pi}{4} \right), \quad \mu > 0. \quad (4.18)$$

### 4.3 DDP method

In the early 1960s, A. M. Dykhne considered the problem of calculating transition probabilities for discrete spectrum states of a system evolving under adiabatic conditions [13, 14]. The treatment was quite general, the main assumptions of Dykhne were that the Hamiltonian was analytic in time and that the transition was localised near the crossing points of the adiabatic energies where it would be sufficient to consider only the leading terms of the adiabatic energies and non-adiabatic coupling between the states. As discussed, these zero points lie in general in the complex time plane. This resulted in a well-known approximative formula for transition probability  $P$ :

$$P = \exp \left[ -2\text{Im} \int_0^{t_c} (E_2(s) - E_1(s)) ds \right]. \quad (4.19)$$

The Dykhne formula, also often called Landau-Dykhne formula, is in general a good approximation when the crossings are located far from the real axis. This is true when the separation of the energy levels or the time scale on which the Hamiltonian is changing is large [36]. Indeed, the rigorous proof of the Dykhne formula was given by Davis and Pechukas in the adiabatic limit [15]. Of course, the formula may give good results also in some situations beyond the adiabatic limit. For example, it can be shown to give the exact result for the Landau-Zener model [36].

Davis and Pechukas also made the idea of Dykhne more clear with a simple formulation in terms of complex contour integration. Therefore this approximation method is often called the Dykhne-Davis-Pechukas method or more concisely as the DDP method.

The result (4.19) is rather non-intuitive in the sense that it depends only on the eigenenergies of the states and does not contain the non-adiabatic coupling that causes the transition. Moreover, it may seem somewhat paradoxical that one can use the adiabatic theorem in the complex plane to get the non-adiabatic transitions in the real-line [37]. To clarify these things, the DDP method is discussed here in

detail, following mostly the formulation of Davis and Pechukas in [15] and then it is applied to the parabolic model.

Davis and Pechukas used the adiabatic basis in their treatise and we use here the notation that was introduced in the context of the change of basis in the section 1.4 with the exception that we choose to write explicitly in the place of the reduced Planck constant  $\hbar$  a parameter  $\lambda$  in the equations. For example, the wavefunction in the adiabatic basis is written as

$$|\Psi(t)\rangle = a_1(t)e^{-i\int_0^t E_1(s)ds/\lambda}|\chi_1(t)\rangle + a_2(t)e^{-i\int_0^t E_2(s)ds/\lambda}|\chi_2(t)\rangle. \quad (4.20)$$

This is because of the fact that when the adiabaticity parameter, now  $\lambda$ , appears just as a scaling of time  $\lambda t \leftrightarrow t$ , the parameter takes the place of  $\hbar$ , so that the adiabatic limit  $\lambda \rightarrow 0$  is equivalent for taking the limit  $\hbar \rightarrow 0$ . Davis and Pechukas therefore identify the adiabatic and the semiclassical limit to be the same although strictly speaking this is not always the case despite the scaling argument. The Hamiltonian still conceals an  $\hbar$ -dependence which is different for different cases [38]. Also, the differential equations for the amplitudes  $a_1(t)$  and  $a_2(t)$  are now given similarly as in the equation (1.46):

$$\dot{a}_1 = -\gamma e^{-i\Delta/\lambda}a_2, \quad \dot{a}_2 = \gamma e^{i\Delta/\lambda}a_1, \quad (4.21)$$

where the  $\gamma(t)$  is the non-adiabatic coupling, and  $\Delta(t)$  is as defined in the equation (1.47) and we choose  $E_2(t) > E_1(t)$  when  $t$  is real.

### 4.3.1 Analytic behaviour of the eigenvalues

It was assumed in the treatise of the problem by Davis and Pechukas that the diabatic Hamiltonian  $\mathbf{H}(t)$  is a symmetric  $2 \times 2$ -matrix, real valued for real  $t$  and that it is analytic and single valued in  $t$  throughout a region of the complex plane from the real axis to the complex crossing point which is closest to the real axis. The exact specification of this region is done by requiring that it contains a certain

level line which is to be discussed soon. The imposed assumptions are equivalent to that the elements of the matrix fulfill these conditions.

The analyticity allows one to use the Cauchy integral theorem which states that for a function  $f(z)$ , which is analytic in a region of the complex plane containing a closed curve  $\mathcal{C}$ , the integration along any such curve will always yield

$$\oint_{\mathcal{C}} f(z)dz = 0. \quad (4.22)$$

Therefore, one can choose a contour, denoting it with  $\mathcal{C}_c$ , on the complex plane so that if it is connected to the real axis at the both ends of the real line and it lies in the region where the function was assumed to be analytic, one can solve an integration with respect to real time with the help of integration along the contour  $\mathcal{C} = \mathcal{C}_r + \mathcal{C}_c$  where  $\mathcal{C}_r$  denotes the real axis, so that

$$\int_{\mathcal{C}_r} f(z)dz = - \int_{\mathcal{C}_c} f(z)dz \quad (4.23)$$

$$= \int_{-\mathcal{C}_c} f(z)dz. \quad (4.24)$$

The curve  $-\mathcal{C}_c$  is the originally chosen curve  $\mathcal{C}_c$  but traversed in the opposite direction. We wish to solve the time evolution of the system by integrating along the level lines of the eigenvalues which are continued analytically to the complex plane, as discussed below. Of course, when modifying the integration path to the complex plane, one loses the detailed information about the time evolution of the system in the real line. That is, the method is only used to solve the asymptotic evolution of the system.

The separation of the energy eigenvalues is now

$$\delta E(t) = \sqrt{(H_{11} - H_{22})^2 + 4H_{12}^2}, \quad (4.25)$$

so that crossing points  $t_c$  are the zero points of this equation:

$$H_{11}(t_c) - H_{22}(t_c) = \pm 2iH_{12}(t_c). \quad (4.26)$$

Therefore the number of complex crossing points in general is even. In the region where the Hamiltonian was assumed to be analytic and single valued, all the possible singularities of the eigenvalues are the branch points that follow from square root term in the eigenvalue function. Moreover, the right and left hand sides of the equation (4.26) do not in general both vanish at the crossing point and the derivative of  $\delta E(t)^2$  is in general non-zero at the crossing. Then one can write in the neighbourhood of  $t_c$

$$\delta E(t) = A\sqrt{t - t_c}[1 + \beta(t)(t - t_c)], \quad (4.27)$$

where  $A$  is constant and  $\beta(t)$  is analytic and single-valued around the crossing point. Now going around  $t_c$  once  $\delta E(t)$  changes to  $-\delta E(t)$ , due to the fact that the complex square root function present in the equation (4.27) is not a single-valued function but has a branch point at  $t_c$ , and therefore the eigenvalues exchange their labels. If however, at least the first derivative of  $\delta E(t)^2$  is zero at  $t_c$ , (4.26) would vanish at  $t_c$  as  $(t - t_c)^{\frac{n}{2}}$  for some  $n$ . If it is odd, we still have a branch point at  $t_c$ . Otherwise there is no branch point and the eigenvalues cross without the exchange of the labels. For our purposes it is sufficient to have  $n = 1$ .

The structure of the complex crossing points could be quite intricate in general. However, the one closest to the real axis dominates the non-adiabatic transition so it is sufficient to consider only that one. It is assumed that the crossing point lies off the real axis at all times so that there is no eigenvalue crossing, not even at the endpoints  $t \rightarrow \pm\infty$ . Moreover, as discussed, the crossing points are located symmetrically with respect to imaginary axis and we choose to consider the one that is on the upper half of the complex plane. There can also be many crossing points equally far from the real axis but at the time being we assume that only one such point exists and generalize the method for the case of several points later.

A *level line* is defined as a curve on the complex plane for which  $Im\Delta(t) = C$ , where  $C$  is constant. As we are considering only the upper half of the complex plane,

$C$  is positive. The level lines near the real axis can be computed approximatively by writing  $t = x + iy$  and then approximating the equation (1.47) for small  $y$  as

$$\Delta(x + iy) \approx \int_0^x \delta E(s) ds + iy \delta E(x). \quad (4.28)$$

Now the equation for the level lines with small  $C$  reads

$$y(x) \approx C/\delta E(x). \quad (4.29)$$

The eigenvalues are real always when  $t$  is real, so then  $C = 0$  and the real line is also a level line. When constructing the other level lines by increasing  $C$  one eventually finds a value where the level line goes through the crossing point  $t_c$  nearest to the real line so that  $Im\Delta(t_c)$  is smallest. From equation (4.27) it follows that near  $t_c$  we have

$$\Delta(t) \approx \Delta(t_c) + \frac{2A}{3}(t - t_c)^{\frac{3}{2}} \quad (4.30)$$

and the level line that passes the crossing point will split at  $t_c$  into three different lines of constant  $Im\Delta(t)$  with  $2\pi/3$  angles between them.

The function  $\theta(t)$  is singular at  $t_c$  because from its definition in the equation (1.38) and from the equations (4.25) and (4.27) it follows that when  $t$  tends to  $t_c$  we have

$$e^{2i\theta} \sim \delta E(t)^{\pm 2} \sim (t - t_c)^{\pm 1}, \quad (4.31)$$

and

$$\frac{\dot{\theta}(t)}{2} \sim \pm \frac{1}{4i(t - t_c)}. \quad (4.32)$$

The function  $\dot{\theta}(t)$  is analytic when  $t \neq t_c$  so by fixing the sign of the adiabatic basis vectors we have in the neighborhood of the crossing point

$$\gamma(t) = \frac{1}{4i(t - t_c)} + \eta(t), \quad (4.33)$$

where the function  $\eta(t)$  is analytic at  $t_c$ . It is seen from this that the leading term of the non-adiabatic coupling has a simple pole at  $t_c$  and the residue is independent of



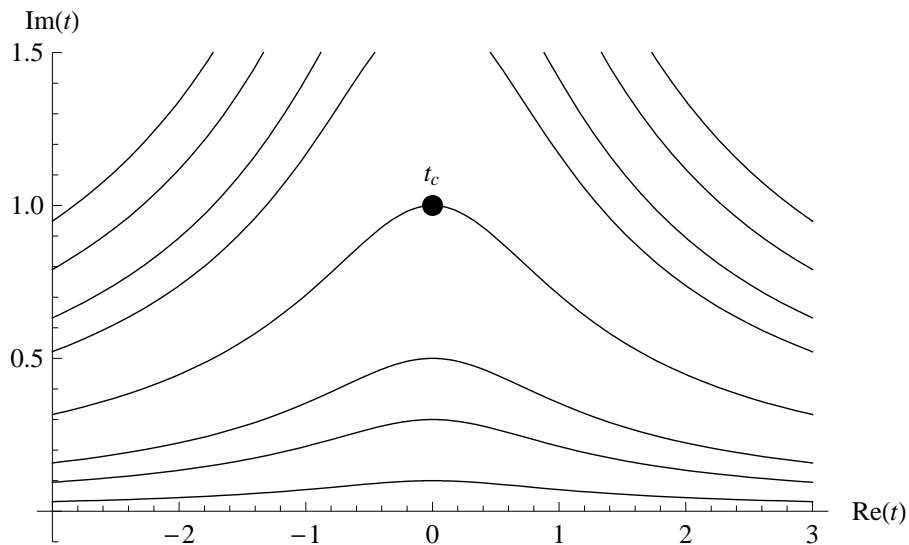


Figure 4. A few of the level lines for  $Im\Delta(t)$  in the upper half of the complex plane in the case of a single crossing as in the Landau-Zener model.

the form of the Hamiltonian. This explains the non-intuitive feature of the Dykhne formula because it shall be shown here that in the adiabatic limit all the contribution to the calculations comes from the vicinity of the crossing point. So the Dykhne formula does not imply that the non-adiabatic coupling does not matter but that the leading term of the coupling is same for all cases.

### 4.3.2 Crossing point dominance

If the non-adiabatic coupling  $\gamma(t)$  goes to zero when  $|t| \rightarrow \infty$  the integration path can be modified from the real line to the level line which passes the complex crossing point except that the crossing point itself must be circled from below along an arc which satisfies  $|t - t_c| = C\lambda^{2/3}$  in order to avoid the branch point  $t_c$ . The integral is split into three parts: the first part is the integration from the left end of the contour along the level line to a point  $t_-$  (see fig. 5), the center part is from  $t_-$  to  $t_+$  which also includes the detour below  $t_c$ , and the third part is from  $t_+$  to the right end of the contour. It is now shown that only the center one of the three parts contribute to the integral in the adiabatic limit. We slightly redefine the amplitudes

of the vectors in the adiabatic basis as

$$\tilde{a}_2 = e^{-i\Delta_c/\lambda} a_2, \quad \tilde{a}_1 = a_1, \quad (4.34)$$

where  $\Delta(t_c) \equiv \Delta_c$ . The differential equations (4.21) are now

$$\dot{\tilde{a}}_2 = \gamma e^{i(\Delta-\Delta_c)/\lambda} \tilde{a}_1, \quad \dot{\tilde{a}}_1 = -\gamma e^{-i(\Delta-\Delta_c)/\lambda} \tilde{a}_2. \quad (4.35)$$

This arrangement ensures that the exponentials are pure phase factors along the level line which passes  $t_c$ , that is,  $Im(\Delta - \Delta_c) = 0$ . The integral solutions to the equations (4.35) are obtained by partial integration:

$$\begin{aligned} \tilde{a}_2(t, \lambda) &= \tilde{a}_2(-\infty) + \int_{-\infty}^t ds \gamma e^{i(\Delta-\Delta_c)/\lambda} \tilde{a}_1 \\ &= \tilde{a}_2(-\infty) + \lambda \gamma \frac{e^{i(\Delta-\Delta_c)/\lambda}}{i\delta E} \tilde{a}_1 \\ &\quad + i\lambda \int_{-\infty}^t ds \left( \frac{\gamma}{\delta E} \right)' e^{i(\Delta-\Delta_c)/\lambda} \tilde{a}_1 - i\lambda \int_{-\infty}^t ds \left( \frac{\gamma^2}{\delta E} \right) e^{i(\Delta-\Delta_c)/\lambda} \tilde{a}_2, \end{aligned} \quad (4.36)$$

$$\begin{aligned} \tilde{a}_1(t, \lambda) &= \tilde{a}_1(-\infty) - \int_{-\infty}^t ds \gamma e^{-i(\Delta-\Delta_c)/\lambda} \tilde{a}_2 \\ &= \tilde{a}_1(-\infty) + \lambda \gamma \frac{e^{-i(\Delta-\Delta_c)/\lambda}}{i\delta E} \tilde{a}_2 \\ &\quad + i\lambda \int_{-\infty}^t ds \left( \frac{\gamma}{\delta E} \right) e^{-i(\Delta-\Delta_c)/\lambda} \tilde{a}_2 + i\lambda \int_{-\infty}^t ds \left( \frac{\gamma^2}{\delta E} \right) e^{-i(\Delta-\Delta_c)/\lambda} \tilde{a}_1. \end{aligned} \quad (4.37)$$

Considering now the first part of the chosen integration contour, from the left end to point  $t_-$ , let  $M_1$  and  $M_2$  be the least upper bounds of  $|\tilde{a}_1(t) - \tilde{a}_1(-\infty)|$  and  $|\tilde{a}_2(t) - \tilde{a}_2(-\infty)|$ , respectively, when  $t \in (-\infty, t_-)$  and on the contour. It is assumed that  $\gamma$  and  $(\gamma/\delta E)'$  are absolutely integrable. This is not a too restrictive condition, as it is sufficient that those functions go to zero faster than  $|t|^{-1}$ . It is then easy to see from the integral equations for the amplitudes that

$$\begin{aligned} M_2 &\leq \lambda [(A_1 + A_2)(\tilde{a}_1(-\infty) + M_1) + A_3(\tilde{a}_2(-\infty) + M_2)] \\ M_1 &\leq \lambda [(A_1 + A_2)(\tilde{a}_2(-\infty) + M_2) + A_3(\tilde{a}_1(-\infty) + M_1)], \end{aligned} \quad (4.38)$$

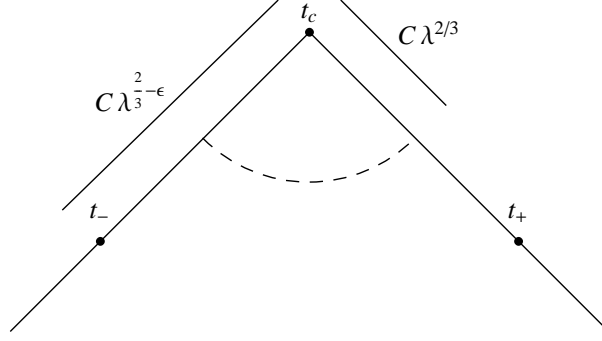


Figure 5. The neighbourhood of the crossing point. Solid line is the level line contour and the dashed arc is the modification made into it in order to avoid the crossing point. The points  $t_-$  and  $t_+$  divide the contour into three parts.

where

$$\begin{aligned}
A_1 &= \max |\gamma(t)/\delta E(t)| \leq |\gamma(t_-)/\delta E(t_c)| \leq C\lambda^{\frac{3\epsilon}{2}-1}, \\
A_2 &= \int_{-\infty}^{t_-} |ds| |(\gamma/\delta E)'| \leq \int_{-\infty}^{t_-} |ds| |s - t_c|^{-5/2}, \\
&\leq C \int_{-\infty}^{t_-} |d|s - t_c| |s - t_c|^{-5/2} \leq C|t_- - t_c|^{-3/2} = C\lambda^{\frac{3\epsilon}{2}-1}, \\
A_3 &= \int_{-\infty}^{t_-} |ds| |(\gamma^2/\delta E)| \leq C \int_{-\infty}^{t_-} |ds| |s - t_c|^{-5/2} \\
&\leq C \int_{-\infty}^{t_-} |d|s - t_c| |s - t_c|^{-5/2} \leq C|t_- - t_c|^{-3/2} = C\lambda^{\frac{3\epsilon}{2}-1}. \tag{4.39}
\end{aligned}$$

Because the numerical value of the constant factor in the bounds is irrelevant here as long as it is finite, we have adopted the notation used by Davis and Pechukas that  $C$  is used in all equations to stand for a bounding constant although their numerical value may be different. This same notation for upper bounds is also used in what follows. Finally, we obtain the bounds for the change of the amplitudes in the first part of the contour as

$$M_i \leq C\lambda^{3\epsilon/2} [\tilde{a}_1(-\infty) + \tilde{a}_2(-\infty)] \leq C\lambda^{3\epsilon/2}, \quad i = 1, 2. \tag{4.40}$$

The same result is obtained for the third part of the contour from  $t_+$  to the right end of the complex plane in a similar way. When  $\lambda \rightarrow 0$  it is seen that the amplitudes

remain constant in these parts of the contour and all of the change in them is confined to the vicinity of the crossing point.

In order to solve the evolution of the system we introduce again the  $S$ -matrix that propagates the system from  $t_-$  to  $t_+$ . The  $S$ -matrix is now defined as

$$\mathbf{S} \equiv \begin{pmatrix} \Omega_- & \Gamma_- \\ \Gamma_+ & \Omega_+ \end{pmatrix}, \quad (4.41)$$

so that

$$\begin{pmatrix} \tilde{a}_1(t_+) \\ \tilde{a}_2(t_+) \end{pmatrix} = \mathbf{S} \cdot \begin{pmatrix} \tilde{a}_1(t_-) \\ \tilde{a}_2(t_-) \end{pmatrix}. \quad (4.42)$$

The matrix elements of the propagator can be expanded as perturbation series,

$$\begin{aligned} \Omega_{\pm} &= 1 - \int_{t_-}^{t_+} dt_1 \gamma e^{\pm i(\Delta - \Delta_c)/\lambda} \int_{t_-}^{t_1} dt_2 \gamma e^{\mp i(\Delta - \Delta_c)/\lambda} + \dots, \\ \Gamma_{\pm} &= \int_{t_-}^{t_+} dt_1 \gamma e^{\pm i(\Delta - \Delta_c)/\lambda} \\ &\quad - \int_{t_-}^{t_+} dt_1 \gamma e^{\pm i(\Delta - \Delta_c)/\lambda} \int_{t_-}^{t_1} dt_2 \gamma e^{\mp i(\Delta - \Delta_c)/\lambda} \int_{t_-}^{t_2} dt_3 \gamma e^{\pm i(\Delta - \Delta_c)/\lambda} + \dots, \end{aligned} \quad (4.43)$$

where the integrations are along the center contour and the series are absolutely convergent.

To actually calculate the elements of the  $S$ -matrix in the adiabatic limit the integrands are split into two parts as

$$\gamma e^{\pm i(\Delta - \Delta_c)/\lambda} = L_{\pm}(t) + R_{\pm}(t), \quad (4.44)$$

where  $L_{\pm}(t)$  is the leading part,

$$L_{\pm}(t) = \frac{e^{\pm 2iA(t-t_c)^{3/2}/3\lambda}}{4i(t-t_c)}, \quad (4.45)$$

and  $R_{\pm}(t)$  is the remainder of the term, explicitly

$$R_{\pm}(t) = \eta(t) e^{\pm i(\Delta - \Delta_c)/\lambda} + L_{\pm}(t) \left[ e^{\pm i \int_{t_c}^t ds A \beta(s) (s-t_c)^{3/2}/\lambda} - 1 \right]. \quad (4.46)$$

The first term of the remainder is bounded because  $\eta(t)$  was analytic at  $t_c$  and the imaginary part of  $\Delta - \Delta_c$  tends to zero as  $\lambda \rightarrow 0$  even in the arc because there we

have  $Im\Delta \leq Im\Delta_c$ . The second term of the remainder is bounded above with the bound

$$\frac{C}{|t-t_c|} \left( e^{C|t-t_c|^{5/2}/\lambda} - 1 \right) \leq \frac{C|t-t_c|^{3/2}}{\lambda} \leq C\lambda^{-3\epsilon/2}, \quad (4.47)$$

and in the center contour we have  $|t-t_c| \leq C\lambda^{2/3-\epsilon}$  so that if  $\epsilon < \frac{4}{15}$  then  $|t-t_c|^{5/2}/\lambda \rightarrow 0$  as  $\lambda \rightarrow 0$ . So now we have an upper limit for the remainder

$$|R_{\pm}(t)| \leq C\lambda^{-3\epsilon/2}, \quad (4.48)$$

and since the length of the center contour is bounded by  $C\lambda^{2/3-\epsilon}$ , the contribution of the remainder term is bounded by

$$\left| \int_{t_-}^{t_+} R_{\pm}(t) dt \right| \leq C\lambda^{2/3-5\epsilon/2}, \quad (4.49)$$

with the above constraint for  $\epsilon$ . Therefore the contribution of the remainder vanishes in the adiabatic limit. If we define a positive constant  $M$  such that

$$|\gamma e^{-i(\Delta-\Delta_c)/\lambda}| \leq |\gamma e^{i(\Delta-\Delta_c)/\lambda}| \leq M, \quad (4.50)$$

then it follows from (4.43) that

$$\begin{aligned} |\Gamma_{\pm}| &\leq M \int_{t_-}^{t_+} |dt_1| + M^3 \int_{t_-}^{t_+} |dt_1| \int_{t_-}^{t_1} |dt_2| \int_{t_-}^{t_2} |dt_3| + \dots \\ &= M \int_{t_-}^{t_+} |dt_1| + \frac{M^2}{3!} \left[ \int_{t_-}^{t_+} |dt_1| \right]^3 + \dots \\ &\leq e^{Ml}, \end{aligned} \quad (4.51)$$

where  $l$  is the total length of the center contour. The upper limit for the matrix elements  $|\Omega_{\pm}|$  is found in a similar way. To calculate the elements it is shown that in the adiabatic limit we can consider only the leading terms. Let

$$\begin{aligned} L(t) &= \max ( |L_+(t)|, |L_-(t)| ), \\ R(t) &= \max ( |R_+(t)|, |R_-(t)| ). \end{aligned} \quad (4.52)$$

By replacing  $|L_{\pm}(t)|$  and  $|R_{\pm}(t)|$  with  $L(t)$  and  $R(t)$  respectively and every  $dt_i$  by  $|dt_i|$  in the perturbation series and finally all minus signs by plus signs we do not

decrease the sum. It follows that we can find an upper limit for  $|\Omega_{\pm}| - |\Omega_{\pm}^0|$  and  $|\Gamma_{\pm}| - |\Gamma_{\pm}^0|$  where  $\Omega_{\pm}^0$  and  $\Gamma_{\pm}^0$  are the series that contain only the leading term in the integrals by

$$\begin{aligned} & \int_{t_-}^{t_+} (L + R)|dt_1| + \int_{t_-}^{t_+} (L + R)|dt_1| \int_{t_-}^{t_1} (L + R)|dt_2| \int_{t_-}^{t_2} (L + R)|dt_3| + \dots \\ & - \int_{t_-}^{t_+} L|dt_1| - \int_{t_-}^{t_+} L|dt_1| \int_{t_-}^{t_1} L|dt_2| \int_{t_-}^{t_2} L|dt_3| - \dots \\ & \leq e^{\int_{t_-}^{t_+} (L+R)|dt|} - e^{\int_{t_-}^{t_+} L|dt|} = e^{\int_{t_-}^{t_+} L|dt|} \left( e^{\int_{t_-}^{t_+} R|dt|} - 1 \right). \end{aligned} \quad (4.53)$$

The term in the parenthesis tends to zero in the adiabatic limit so if  $\int_{t_-}^{t_+} L|dt|$  is bounded it follows that we can consider only the leading terms in the  $S$ -matrix elements in the adiabatic limit. On the center contour we have

$$L(t) \leq \frac{C}{|t - t_c|} \quad (4.54)$$

so therefore

$$\int_{t_-}^{t_+} L(t)|dt| \leq C + C \ln(\lambda^{-\epsilon}), \quad (4.55)$$

and

$$e^{\int_{t_-}^{t_+} L|dt|} \leq C\lambda^{-C\epsilon}, \quad (4.56)$$

which is not bounded when  $\lambda \rightarrow 0$ . However, from the equation (4.49) we have that

$$e^{\int_{t_-}^{t_+} R|dt|} - 1 \leq C\lambda^{2/3-5\epsilon/2}, \quad (4.57)$$

which tends to zero in the adiabatic limit when  $\epsilon < 4/15$ . It follows that for the entire term we have

$$e^{\int_{t_-}^{t_+} L|dt|} \left( e^{\int_{t_-}^{t_+} R|dt|} - 1 \right) \leq C\lambda^{2/3-C\epsilon}, \quad (4.58)$$

which then tends to zero when  $\epsilon$  is chosen small enough depending on the value of the finite constant  $C$ .

To conclude, in the limit  $\lambda \rightarrow 0$  the asymptotic time evolution of the system is obtained by considering the time evolution in the center contour, that is, from  $t_-$  to  $t_+$  with considering only the leading terms in the  $S$ -matrix.

By making a change of variable

$$x \equiv \frac{2A}{3}(t - t_c)^{3/2}, \quad (4.59)$$

it follows from the equations (4.30) and (4.33) that the differential equations (4.35) become

$$\tilde{a}'_1(x) = -\frac{e^{-ix}}{6ix}\tilde{a}_2(x), \quad \tilde{a}'_2(x) = \frac{e^{ix}}{6ix}\tilde{a}_1(x), \quad (4.60)$$

where ( $'$ ) stands for derivation with respect to the new variable  $x$ . With the initial conditions  $a_1(-\infty) = 1$  and  $a_2(-\infty) = 0$  we have the integral equations

$$\tilde{a}_2(x) = \int_{-\infty}^x dx' \frac{e^{ix'}}{6ix'} \tilde{a}_1(x'), \quad (4.61)$$

$$\begin{aligned} \tilde{a}_1(x) &= 1 - \int_{-\infty}^x dx' \frac{e^{-ix'}}{6ix'} \tilde{a}_2(x') \\ &= 1 + \left(\frac{1}{36}\right) \int_{-\infty}^x dx' \frac{e^{-ix'}}{x'} \int_{-\infty}^{x'} dx'' \frac{e^{ix''}}{x''} \tilde{a}_1(x''). \end{aligned} \quad (4.62)$$

Because  $e^{i\Delta_c/\lambda}$  was independent of the particular Hamiltonian in the adiabatic limit the matrix elements could be actually calculated by referring to some appropriate solvable two-state model such as the Landau-Zener model or it could be integrated directly by considering only the leading terms around  $t_c$ . However, Davis and Pechukas perform and justify a more elementary-looking but somewhat tricky manoeuvre. They compute an asymptotic expansion for  $\tilde{a}_1$  with large  $x$  as

$$\tilde{a}_1(x) \sim \sum_{n=0}^{\infty} \frac{\alpha_n n!}{(ix)^n}, \quad \alpha_0 = 1. \quad (4.63)$$

Inserting the expansion in the integral equation and then by repeated integration the recurrence relation

$$\alpha_n = -\frac{1}{36n^2} \sum_{m=0}^{n-1} \alpha_m \quad (4.64)$$

is obtained. Now by setting  $\beta_n = -36n^2\alpha_n$ ,  $n \neq 0$  it follows from the equation (4.64) that  $\beta_{n+1} = (1 - 1/36n^2)$  and since  $\beta_1 = 1$  we have

$$\beta_n = \prod_{m=1}^{n-1} \left(1 - \frac{1}{36m^2}\right). \quad (4.65)$$

If the series (4.63) is inserted in the integral equation for  $\tilde{a}_2$  the repeated partial integration gives the asymptotic amplitude as

$$\tilde{a}_2(\infty) = \left(\frac{\pi}{3}\right) \sum_{m=0}^{\infty} \alpha_m = \left(\frac{\pi}{3}\right) \lim_{n \rightarrow \infty} \beta_n = \left(\frac{\pi}{3}\right) \prod_{m=1}^{\infty} \left(1 - \frac{1}{(6m)^2}\right) = 1, \quad (4.66)$$

where in the last steps we have used the equations (4.64), (4.65) and an infinite product representation [23]

$$\frac{\sin(z)}{z} = \prod_{m=1}^{\infty} \left(1 - \frac{z^2}{(6m)^2}\right). \quad (4.67)$$

Now we have calculated the matrix element  $\Gamma_+$  because with the chosen initial conditions  $\tilde{a}_1(-\infty) = 1$ ,  $\tilde{a}_2(-\infty) = 0$  and the definition of the  $S$ -matrix we get  $\tilde{a}_2(\infty) = \Gamma_+ = 1$ .

The other matrix elements can be obtained more easily. By considering the initial conditions and the adiabatic theorem we know that  $\tilde{a}_1(\infty) \rightarrow 1$  when  $\lambda \rightarrow 0$  and furthermore we know that the amplitudes are asymptotically constant everywhere except in the center contour so that  $\tilde{a}_1(t_+) \rightarrow 1$ ,  $\tilde{a}_1(t_-) \rightarrow 1$  and  $\tilde{a}_2(t_-) \rightarrow 0$  as  $\lambda \rightarrow 0$ . It follows that  $\Omega_- \rightarrow 1$ . The rest of the elements are obtained considering the inverse of the  $S$ -matrix defined in equation (4.42). Although this time due to approximate nature of the calculations we did not define the  $S$ -matrix to be strictly unitary it is assumed to have an inverse, a condition for this is now  $\Omega_+ \neq \Gamma_-$ . The elements of the inverse can be calculated from the equation (4.43) by interchanging the limits of integration where it follows that we have

$$\begin{pmatrix} \tilde{a}_1(t_-) \\ \tilde{a}_2(t_-) \end{pmatrix} = \begin{pmatrix} \Omega_- & -\Gamma_- \\ -\Gamma_+ & \Omega_+ \end{pmatrix} \begin{pmatrix} \tilde{a}_1(t_+) \\ \tilde{a}_2(t_+) \end{pmatrix}. \quad (4.68)$$

so that

$$\begin{pmatrix} \Omega_- & \Gamma_- \\ \Gamma_+ & \Omega_+ \end{pmatrix} \begin{pmatrix} \Omega_- & -\Gamma_- \\ -\Gamma_+ & \Omega_+ \end{pmatrix} = \begin{pmatrix} 1 & 0 \\ 0 & 1 \end{pmatrix}, \quad (4.69)$$

which can be solved with the help of the already solved matrix elements  $\Gamma_+$  and  $\Omega_-$  which result in  $\Gamma_- \rightarrow 0$  and  $\Omega_+ \rightarrow 1$  as  $\lambda \rightarrow 0$ .



Now returning from the redefinition of equation (4.34) to the original definition of the amplitudes we have finally obtained an equation for the amplitudes in the case of a single crossing as

$$\begin{pmatrix} a_1(\infty) \\ a_2(\infty) \end{pmatrix} = \begin{pmatrix} 1 & 0 \\ e^{i\Delta_c} & 1 \end{pmatrix} \begin{pmatrix} a_1(-\infty) \\ a_2(-\infty) \end{pmatrix}. \quad (4.70)$$

It should be noted that although often in practise one has to use numerical methods anyway because the eigenvalue functions may be complicated or because one has to go beyond the approximation of equation (4.29), the numerical integration to obtain the term  $e^{i\Delta_c}$  is still much faster than solving the whole Schrödinger equation numerically.

### 4.3.3 Parabolic model in the DDP approximation

Davis and Pechukas discussed shortly also generalisations of their method and suggested that for the case of several complex crossing points on the level line, one can add up the contributions calculated separately from each of the crossing point as a coherent sum. When applying this for the double crossing case in the parabolic model we have to be aware of the fact that the non-adiabatic coupling is in that case an antisymmetric function of time,  $\gamma(-t) = -\gamma(t)$ . In the derivation of the DDP method we fixed the non-adiabatic coupling by choosing the positive sign in equation (4.33) but now we can not choose the sign for the both crossing point independently. We can take this into account by fixing the sign in the first crossing point and then placing a minus sign in front of the exponential term  $e^{i\Delta_c^{(2)}}$  in the second crossing point. Therefore the final populations for the double crossing case are obtained from the equation

$$\begin{pmatrix} a_1(\infty) \\ a_2(\infty) \end{pmatrix} = \begin{pmatrix} 1 & 0 \\ e^{i\Delta_c^{(1)}} - e^{i\Delta_c^{(2)}} & 1 \end{pmatrix} \begin{pmatrix} a_1(-\infty) \\ a_2(-\infty) \end{pmatrix}. \quad (4.71)$$

The complex crossing points  $\tau_c^{(i)}$  were calculated already in the equation (3.4) and now considering only the ones with positive imaginary part we have

$$\Delta_c \equiv \Delta_c^{(2)} = - [\Delta_c^{(1)}]^* = \frac{2}{\sqrt{\epsilon}} \int_0^{x_c^{(2)}/\sqrt{\epsilon}} dx \sqrt{1 + (\mu - x^2)^2}, \quad (4.72)$$

where we already have scaled the integration variable in the integral over the eigenenergies as  $x \equiv \sqrt{\epsilon}\tau$ . The integrals of the form  $\Delta_c$  appearing in the previous formulas can be calculated with the help of the change of variables  $x \equiv \sqrt{i + \mu} \sin \vartheta$  and then using the binomial series as done in the reference [32] to obtain

$$\Delta_c = \frac{2}{\sqrt{\epsilon}} e^{i\pi/4} (1 - i\mu)(1 + i\mu)^{1/2} \int_0^{\pi/2} d\vartheta \cos^2(\vartheta) \left( 1 + \frac{(1 - i\mu) \sin^2(\vartheta)}{1 + i\mu} \right)^{1/2}. \quad (4.73)$$

This can be solved with a further substitution  $\sin^2 \equiv t$  and then using the equation (15.3.1) of the reference [22] we get

$$\Delta_c = \frac{\pi}{2\sqrt{\epsilon}} \sqrt{(\mu + i)(\mu^2 + 1)} {}_2F_1 [1/2, -1/2; 2; z(\mu)], \quad (4.74)$$

where we again have the hypergeometric function, now with the variable

$$z(\mu) = \frac{\mu + i}{\mu - i} = \left( \frac{\mu + i}{\sqrt{1 + \mu^2}} \right)^2. \quad (4.75)$$

The straightforward application of equation (4.71) with the usual initial conditions  $|a_1(-\infty)| = 1$  and  $a_2(-\infty) = 0$  gives

$$\begin{aligned} a_2(\infty) &= (e^{i\Delta_c^{(1)}} - e^{i\Delta_c^{(2)}}) a_1(-\infty) \\ &= (e^{-i\Delta_c^*} - e^{i\Delta_c}) a_1(-\infty) \\ &= -2ie^{-Im\Delta_c} \sin(Re\Delta_c) a_1(-\infty), \end{aligned} \quad (4.76)$$

and now denoting the asymptotic probability for the amplitude in this case by  $|a_2(\infty)|^2 \equiv P_1^{DDP}$  we get

$$P_1^{DDP} = 4 \sin^2(Re\Delta_c) e^{-2Im\Delta_c}. \quad (4.77)$$

#### 4.4 The modified DDP method

The DDP method can be in general expected to give good results only near the adiabatic limit. To be able to give good approximations of the populations for parameters outside adiabatic regions we modify this method by including the phase term given in the context of the independent crossing approximation and the Landau-Zener model by the equation (4.8). The DDP method itself does not give this phase term but it does give of course the normal phase evolution of the system even when  $\mu \approx 0$ , that is when the crossings overlap and treating the system as a double Landau-Zener model as in section 4.1 does not work. Therefore, the modified DDP method covers a larger part of the parameter region of the parabolic model than the independent crossing approximation.

The procedure here is very similar to what is done in the independent crossing approximation but now our  $S$ -matrix to be applied twice is given by the DDP method for a single crossing and therefore by the equation (4.70). The inclusion of the extra phase term is done by inserting the term  $e^{-i\chi}$  into the upper corner of the  $S$ -matrices. Now with the same initial conditions and similar calculations as in the equation (4.76) we get the final result as

$$P_1^{DDPm} = 4 \sin^2 (Re\Delta_c + \chi) (1 - e^{-2Im\Delta_c}) e^{-2Im\Delta_c}. \quad (4.78)$$

## 5 Numerical studies

Numerical methods were used to solve the parabolic model in order to use the results as a benchmark for the different approximative expressions obtained in the previous section. The two coupled first-order differential equations arising from the time-dependent Schrödinger equation were solved numerically with different parameter regions so that the comparison between different approximations and finding their regions of applicability is possible.

The implementation of the numerical calculations were done with Mathematica 6.0 software [39] by constructing a simple program that makes use of the NDSolve routine of Mathematica. NDSolve is a numerical differential equation solver and although the routine offers many options concerning for example the method of solving or the precision or the stepsize to be used, it still has a certain "black box" character and therefore one has to take a critical look at the results it gives and somehow ensure their correctness. In our case there actually already exists previous numerical results for the parabolic model obtained by using the Runge-Kutta method to solve the Schrödinger equation in a quite wide parameter region [28]. By using the same parameters we obtained results that were in a good agreement with those given in the reference and this gives confidence to our numerical studies. When comparing the results, one should note anyhow that the reference [28] contains some misprints and for example the numerical simulation for the case  $\mu = 10$  in the reference [28] is more likely to be really the case where the parameter value is  $\mu = 5$  [40] so also that case fits perfectly to our results.

The program that was used calculated numerically the solutions to the coupled differential equations to give the final amplitudes in the diabatic basis with the same initial conditions used in the previous section. So although we used only the final state of the system and the values it gives for the amplitudes of the basis states the whole time evolution of the system had to be of course calculated. In each run of the

program we kept either  $\epsilon$  or  $\mu$  fixed and computed the final probability distributions while varying the other parameter. For example, to determine the  $\epsilon$ -dependence of the probability distributions for a parabolic model in a highly tunneling case one would fix the  $\mu$  to be for example  $\mu = -5$  and then run the program which would solve the differential equations in a sufficiently large region, for example  $\epsilon \in [0, 100]$ . In practise of course the calculations are done for close-lying but discrete values of  $\epsilon$  on the interval  $[0, 100]$ . From these solutions the population is computed at the end of the interval and finally a curve is fitted to these values so that the  $\epsilon$ -dependence of the final population is obtained.

Another practical issue in numerical studies is of course that the time interval can not be taken to be infinite but has to be bounded by some value that is large enough to keep the error small. The change of the probability amplitudes is concentrated near the crossings and therefore usually near the origin as discussed earlier. An example of this behaviour can be seen from the figure 6. Therefore sufficiently small time intervals are needed in many cases. However, when the system tends to more and more adiabatic parameter regions one should correspondingly take the time interval to be longer and longer which causes problems because the size of the timestep has to be kept small anyway. Also, the rapid oscillations in the final populations lead to difficulties. This happens, for example, when  $\mu$  is positive and large. Then to obtain a good fit for the probabilities one has to make the spacing of the discrete values of  $\epsilon$  more dense and therefore the calculations get more time-consuming.

One challenge for the numerical studies is that the needed time interval and the spacing of the sample values for the parameter that is not fixed beforehand changes during the run of the program and depends on the value of the other, fixed parameter. However, even without a general formula for doing this one obtains quite easily sufficient estimations for needed values in each of the parameter regions.

The results of numerical simulations are presented in the section 7 together with the comparison of the different approximative results. However, in order to illustrate the things discussed here, we have plotted in the figure 6 the time evolution of the transition probability for some of the individual amplitudes with different parameters. We have also included the values that the most suitable approximative results in each region give for the final transition probabilities. The parameter  $\mu$  is fixed to unity while  $\epsilon$  is plotted for three values, 1, 5 and 20. There one can see some of the characteristic behaviour. The topmost plot is the most adiabatic one with  $\epsilon = 1$  and although the transition probability goes to almost unity near the temporal zero point it dies out with some oscillations and has a small final value. In the next plot we have  $\epsilon = 5$  and a complete population transfer. The change in the amplitudes is also somewhat more concentrated in the vicinity of the origin. In the lowest picture we have  $\epsilon = 20$  and it can be seen that the final transition probability does not grow monotonically with  $\epsilon$ ; now we have  $P \approx 0.6$ . Also, in the undermost plot one should note that none of the approximations gives a sensible answer.

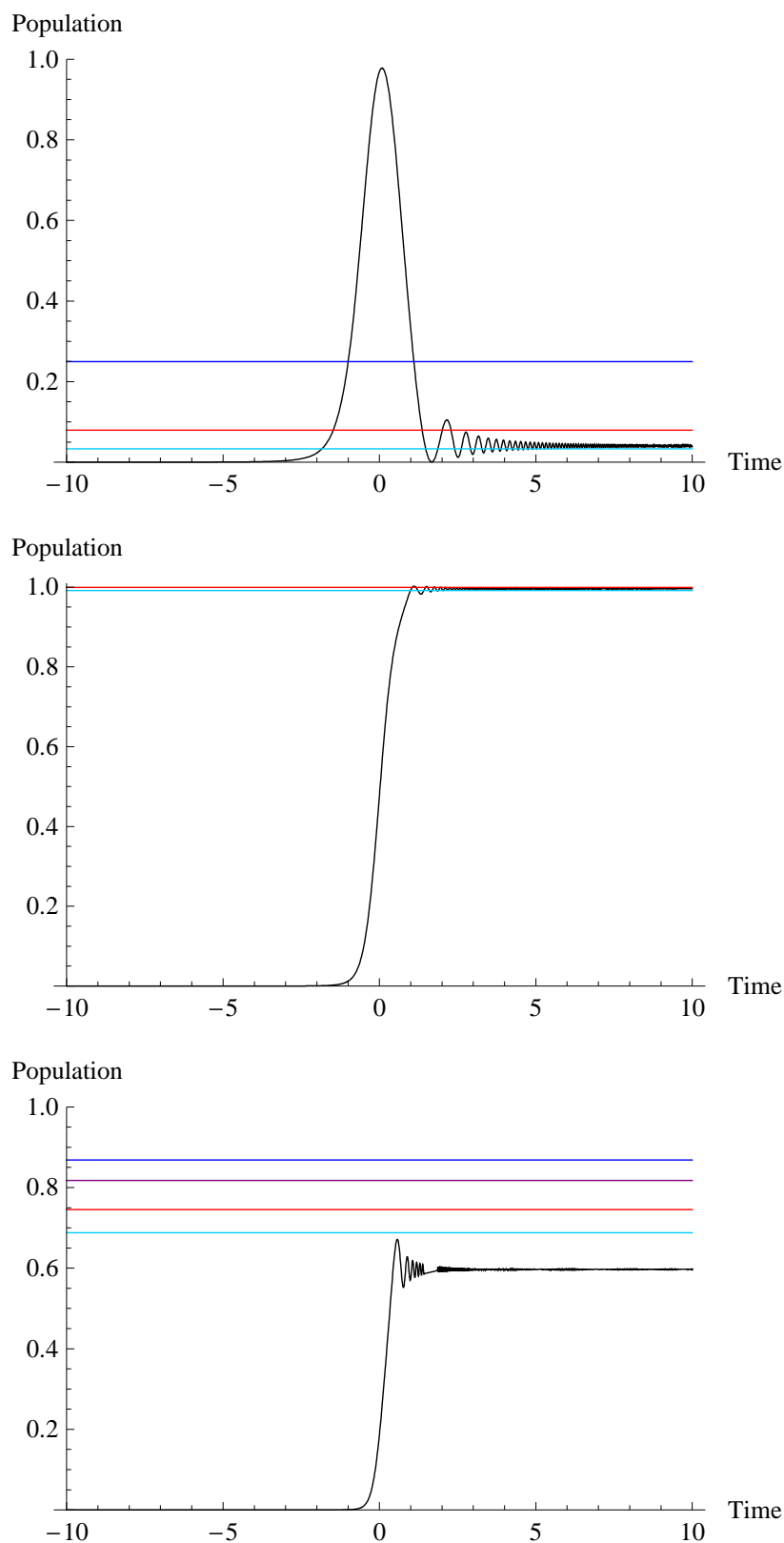


Figure 6. The numerical solution of  $P_1(t)$  plotted as solid blue line for three different parameters, from top:  $\epsilon = 1$ ,  $\epsilon = 5$  and  $\epsilon = 20$  with  $\mu = 1$  in all of them. Also plotted are the values of the asymptotic transition probabilities given by those approximation methods that give sensible results in these cases. The red solid line is the independent crossings approximation while the purple line is the perturbation result. The values obtained with the pure and the modified DDP method are given by dark and light blue lines, respectively.

## 6 Results of Shimshoni and Gefen

Although we already obtained various approximative results to the parabolic model we study the problem in this section once more and from a little bit different angle. All the approximative methods that were used were given in the adiabatic basis, except the perturbation approach. As discussed, in principle there is no preference between the bases and because the asymptotic basis states are the same for adiabatic and diabatic basis states in the parabolic model the asymptotic transition probability could be given simultaneously in both bases. However, we also noted that the expressions that were obtained for phases in different bases were different. An example of this was seen in the context of independent crossing approximation. The correct calculations of the phase terms are of crucial importance in the parabolic model where the phases contribute directly to the transition probability.

Shimshoni and Gefen have studied the parabolic model and calculated asymptotic transition probabilities in different parameter regions in [41]. They were interested in the dephasing and relaxation of an externally driven system coupled to an environment and in this context considered the coherence properties of non-adiabatic transitions. Despite some similarities with the approximative results obtained above, in general their results seemed to differ. They used in their calculations interchangeably either the diabatic or the adiabatic bases in appropriate parameter regions as was suggested to be desirable in the section 1.4. The results were obtained both in the diabatic and the adiabatic limits first by considering two independent Landau-Zener crossings and then with a more general calculation using the actual parabolic model.

The objective here is to clarify and understand the differences of the different results and to see if the results obtained by their method or the ones used above are in a considerably better agreement with the numerical results at least in some parameter regions. We do this below by reviewing their calculation and comparing



the results.

## 6.1 The independent crossing approximation

The independent crossing approximation was already discussed quite thoroughly in the section 4.1. The idea here is equivalent to that and we outline only the calculations to derive the scattering matrix and the phase terms for a single Landau-Zener transition using the same notation as before whenever possible.

Shimshoni and Gefen derived the scattering matrix elements in the form

$$S_1 = \sqrt{1 - R^2} e^{i\theta_1}, \quad S_2 = R e^{i\theta_2}, \quad (6.1)$$

where  $R = e^{-\pi\Lambda_{\text{eff}}/2}$  was defined in the section 2 and the arguments of the phases,  $\theta_i, i = 1, 2$  are the important quantities whose values are to be specified here. They may depend on different parameters but calculating them is quite easy, at least in the diabatic and adiabatic limits. With the usual initial conditions  $C_-(-\infty) = 0$  and  $C_+(-\infty) = 1$  the asymptotic transition probability is obtained in the same way as in the equation (6.2),

$$\tilde{P}_1^{\text{LZ}} = 4e^{-\pi\Lambda_{\text{eff}}} (1 - e^{-\pi\Lambda_{\text{eff}}}) \sin^2(\phi + \theta_1), \quad (6.2)$$

where the tilde is used to distinguish the results of Shimshoni and Gefen from the ones obtained above with similar approximations.

Considering first the Landau-Zener model and the diabatic approximation we use the diabatic basis so that every vector can be written as

$$|\psi(t)\rangle = C_-(t)e^{-i\phi(t)}|-\rangle + C_+(t)e^{i\phi(t)}|+\rangle, \quad (6.3)$$

where  $\phi(t)$  is the diabatic dynamical phase given by the equation (3.7). Using the same form of the time-dependent Schrödinger equation as in [1] we obtain a pair of coupled differential equations as before but now they reduce to the form

$$\dot{C}_{\mp}(t) = iV e^{\pm i\lambda t^2} C_{\pm}(t). \quad (6.4)$$

In the diabatic approximation and using the same parameter  $\Lambda \equiv V^2/\lambda$  defined already for the Landau-Zener model we now have the condition  $\Lambda \ll 1$ . Shimshoni and Gefen introduced a similar but not yet equivalent scaling of time as in (2.4), namely  $y = t\sqrt{2\lambda}$ , and obtained

$$\frac{dC_{\mp}(y)}{dy} = i\sqrt{\frac{\Lambda}{2}}e^{\pm iy^2/2}C_{\pm}(y). \quad (6.5)$$

The parameter  $\Lambda$  is small and the solution of (6.5) is expanded as a power series in  $\sqrt{\Lambda}$ ,

$$C_{\pm}(y) = \sum_{n=0}^{\infty} C_{\pm}^{(n)}(y)\Lambda^{n/2}. \quad (6.6)$$

The amplitudes  $C_{\pm}(\infty)$  are then calculated in the lowest order in  $\sqrt{\Lambda}$ . From the initial conditions it follows that we must have  $C_{-}^{(0)} = 0$  and  $C_{+}^{(0)} = 1$ . Inserting the power series in the differential equation (6.5) and considering only the lowest terms we get

$$C_{-}(\infty) = i\sqrt{\frac{\Lambda}{2}} \int_{-\infty}^{\infty} e^{iy^2/2} dy = i\sqrt{2\Lambda} \int_0^{\infty} e^{iy^2/2} dy. \quad (6.7)$$

Integrating the above integral in the right-hand side of (6.7) is equal to integrating along the line  $y = xe^{i\pi/4}$ . Therefore we end up with a Gaussian integral and the result

$$S_1 = 2i\sqrt{\Lambda}e^{i\pi/4} \int_0^{\infty} e^{-x^2/2} dx = \sqrt{\pi\Lambda}e^{i3\pi/4}. \quad (6.8)$$

The Landau-Zener factor can be given as series so for small  $\Lambda$  it suffices to keep only the terms up to first order in  $\Lambda$ . Then by comparing the expressions (6.1) and (6.8) we see that in the diabatic limit we have  $\theta_1 = 3\pi/4$ .

$C_{+}(\infty)$  is obtained similarly by substituting the power series into the differential equation and considering the initial conditions. Due to the fact that  $C_{-}^{(0)} = 0$  the result is to second order in  $\sqrt{\Lambda}$  and we get

$$S_2 = 1 - \frac{\pi\Lambda}{2}, \quad (6.9)$$

and now a comparison between the expressions implies that in the diabatic limit  $\theta_2 = 0$  although, with the chosen initial conditions, this phase term does not contribute to the transition probability anyway.

Next we study the adiabatic limit. Shimshoni and Gefen used some of the methods and analytical considerations originally used in the references [15] and [42] to solve the adiabatic case and therefore also implicitly using the same main assumptions as the DDP method. However, as they are only interested in the Landau-Zener and the parabolic models where these assumptions are valid they do not state them explicitly. In any case, it is seen that there is a connection with the methods they use and with those we have used to derive our main results as presented before in this thesis.

In the adiabatic limit we use the adiabatic basis and write the state vector in it as

$$|\psi(t)\rangle = a_1(t)e^{i\phi_1^a(t)}|\chi_1(t)\rangle + a_2(t)e^{i\phi_2^a(t)}|\chi_2(t)\rangle, \quad (6.10)$$

where  $|\chi_i\rangle$  and  $\phi_i^a(t)$ ,  $i = 1, 2$  are as before the eigenstates of the system and the dynamic phase accumulated by the the eigenenergies, respectively.

For the initial conditions to be equivalent to those in the diabatic limit it is imposed  $a_2(-\infty) = 0$  and  $a_1(-\infty) = 1$ . With these initial conditions one can approximate in the adiabatic limit  $a_1(t) \approx 1$  for all  $t$  and from the equation (1.46) we have

$$\begin{aligned} a_2(\infty) &\approx \frac{\lambda V}{2} \int_{-\infty}^{\infty} \frac{dt}{(\lambda t)^2 + V^2} \exp \left[ 2i \int_0^t \sqrt{(\lambda t')^2 + V^2} dt' \right] \\ &= \frac{1}{2} \int_{-\infty}^{\infty} \frac{dy}{(1+y^2)} \exp \left[ 2i\Lambda \int_0^y \sqrt{1+x^2} dx \right] \\ &\equiv \frac{1}{2} \int_{-\infty}^{\infty} dw \theta' e^{2i\Lambda w}, \end{aligned} \quad (6.11)$$

where in the second integral time is rescaled by introducing a new variable as  $y = (\lambda/V)t$  and to obtain the solution for the integrals we have finally defined the variable

$$w = \int_0^y dx \sqrt{1+x^2}, \quad (6.12)$$

and the points in the complex plane

$$w_c = \int_0^{y_c} dx \sqrt{1+x^2}, \quad y_c^2 + 1 = 0, \quad (6.13)$$

that is, the points that correspond to the familiar complex zero points of the eigenenergy at  $y_c = \pm i$ . The integrand in the equation (6.11) for the asymptotic amplitude  $a_2(\infty)$  has simple poles in these degeneracy points. Now we again have similarly to the equation (4.30) an expansion near  $y_c$  as

$$w \approx w_c + \frac{2\sqrt{2}}{3}(y - y_c)^{3/2}, \quad (6.14)$$

where the fact that the elements of the Hamiltonian are analytic near the degeneracy points is used. It follows that near  $w_c$  we now have [42]

$$\theta' = \pm \frac{1}{3y_c(w - w_c)}. \quad (6.15)$$

Making the substitutions to equation (6.11) we obtain

$$a_2(\infty) \approx \frac{1}{2} \int_{-\infty}^{\infty} \frac{e^{2i\Lambda w}}{3y_c(w - w_c)} dw. \quad (6.16)$$

From the equation (6.13) we have that the points  $y_c = \pm i$  correspond to  $w_c = \pm i\pi/4$  and they are the poles of the integrand in (6.16). The integrand in equation (6.16) vanishes when the modulus of  $w$  tends to infinity so it is possible to close the integration contour by including a path in the upper half of the complex plane in a such way that it encloses the pole  $w_c = i\pi/4$  but does not change the integral and therefore allows one to use the integral formula of Cauchy [12] to evaluate the integral and we get for the amplitude the result

$$a_2(\infty) \approx \frac{\pi}{3} e^{-\pi\Lambda/2}, \quad (6.17)$$

and for the transition probability

$$|a_2(\infty)|^2 = \left(\frac{\pi}{3}\right)^2 e^{-\pi\Lambda}, \quad (6.18)$$

which indeed provides the Landau-Zener factor in the amplitude but with slightly wrong prefactor  $\pi/3 \approx 1.047$  instead of the normal unity. Neglecting the incorrect prefactor it is seen that the phase terms are zero in the adiabatic limit because in the Landau-Zener model we had the correspondence between the asymptotic states as  $|\chi_1(\infty)\rangle = |-\rangle$  and  $|\chi_2(\infty)\rangle = |+\rangle$  so that in the adiabatic limit the S-matrix element  $S_2$  is exponentially small and  $S_1 \approx 1$  and the phases are  $\theta_1 = \theta_2 = 0$ .

## 6.2 A more general approximative solution

To calculate more detailed and general approximative solution for the asymptotic transition probability of the parabolic model in adiabatic and diabatic limits Gefen and Shimshoni define a parameter which measures the degree of adiabaticity. It is expressed in the scaled variables  $\epsilon, \mu$  and  $\tau$  defined before as  $\delta \equiv 4^{1/3}\epsilon^{-1/3}$  so that  $\delta \rightarrow \infty$  corresponds to the adiabatic limit and  $\delta \rightarrow 0$  to the diabatic limit. Now the differential equations for the amplitudes in the diabatic basis reads

$$\dot{C}_{\mp}(\tau) = ie^{\pm 2i\left(\frac{\epsilon\tau^3}{3} - \mu\tau\right)} C_{\pm}(\tau). \quad (6.19)$$

Let us again scale the time to be dimensionless by the new variable  $y = (2\epsilon)^{1/3}\tau$  and also define  $\tilde{\mu} = \mu/(16\epsilon)^{1/3}$  so that (6.19) becomes

$$\frac{dC_{\mp}(y)}{dy} = i\delta e^{\pm i(y^3/3 - \tilde{\mu}y)} C_{\pm}(y). \quad (6.20)$$

In the diabatic limit the parameter  $\delta$  is small and we again use a power series expansion with respect to this parameter for the solutions  $C_{\pm}(y)$ . Now the assumption that the system is initially in the lower eigenstate corresponds to imposing the initial conditions as  $C_-(-\infty) = 1$  and  $C_+(-\infty) = 0$ . Direct integration yields to first

order in  $\delta$

$$\begin{aligned}
C_+(\infty) &= i\delta \int_{-\infty}^{\infty} e^{-i(y^3/3 - \tilde{\mu}y)} dy \\
&= 2i\delta \int_0^{\infty} \cos(y^3/3 + \tilde{\mu}y) dy \\
&= 2\pi i\delta \text{Ai}(\tilde{\mu}) \\
&= \frac{2\pi i}{\sqrt[3]{2\epsilon}} \text{Ai}\left[-\frac{2\mu}{\sqrt[3]{2\epsilon}}\right], \tag{6.21}
\end{aligned}$$

which is just the same as the perturbation result obtained before. This is obvious because although Shimshoni and Gefen call this result as a sudden approximation the procedure here is similar to a perturbative one, namely expanding the result to power series with respect to small perturbation.

For the adiabatic case where  $\delta \ll 1$  Shimshoni and Gefen use the exactly same method as in the double Landau-Zener approximation. In the parabolic model the correspondence between asymptotic states in the diabatic and adiabatic bases is the same for the initial and final states, meaning that  $|\chi_1(\pm\infty)\rangle = |-\rangle$  and  $|\chi_2(\pm\infty)\rangle = |+\rangle$ . Therefore, the initial conditions are now  $a_1(-\infty) = 1$  and  $a_2(-\infty) = 0$  and the asymptotic transition probability is  $\tilde{P} = |a_2(\infty)|^2$ . As for the Landau-Zener model in the adiabatic case above it is approximated that  $a_1(t) \approx 1$  for all times and we have

$$a_2(\infty) \approx \int_{-\infty}^{\infty} dy \frac{y}{1 + (\mu - y^2)^2} \exp\left[i\delta^{3/2} \int_0^y dx \sqrt{1 + (\mu - x^2)^2}\right], \tag{6.22}$$

with the definition  $y \equiv \sqrt{\epsilon}t$ . We again define a variable with the help of the argument in the exponent:

$$w \equiv \int_0^y dx \sqrt{1 + (\mu - x^2)^2}. \tag{6.23}$$

and the critical complex plane points, there are four of each, are

$$w_c = \int_0^{y_c} dx \sqrt{1 + (\mu - x^2)^2}, \quad y_c = \pm\sqrt{i \pm \mu}. \tag{6.24}$$

Near the critical points  $y_c$  we have

$$w - w_c \approx \frac{4\sqrt{(y_c^2 - \mu)y_c}}{3} (y - y_c)^{3/2} \tag{6.25}$$

and

$$\left(\frac{dw}{dy}\right)^3 \approx 6y_c (y_c^2 - \mu) (w - w_c), \quad (6.26)$$

so that now we have

$$a_2(\infty) \approx \int_{-\infty}^{\infty} \frac{e^{i\delta^{3/2}w} y(w)}{(dw/dy)^3} dw. \quad (6.27)$$

As before, let us consider only the poles in the upper half of the complex plane. Those are the critical points  $y_{c,1} = \sqrt{\mu + i}$  and  $y_{c,2} = -\sqrt{\mu - i}$  and the corresponding points  $w_{c,1}$  and  $w_{c,2}$ . We have the same relations stated before

$$Re(w_{c,1}) = -Re(w_{c,2}), \quad Im(w_{c,1}) = Im(w_{c,2}). \quad (6.28)$$

A similar closing of the integration path as in the Landau-Zener case is done in order to evaluate the integral in equation (6.27). Now the contour encloses a two simple poles  $w_{c,1}$  and  $w_{c,2}$  so by using a generalization of the integral theorem of Cauchy, the residue theorem, we get

$$\begin{aligned} a_2(\infty) &= \frac{\pi}{3} \left[ e^{i\delta^{2/3}w_{c,1}} - e^{i\delta^{2/3}w_{c,2}} \right] \\ &= \frac{\pi}{3} \left[ e^{(i\delta^{2/3}w_{c,1})} - e^{(i\delta^{2/3}w_{c,1})^*} \right] \\ &= \frac{2\pi i}{3} e^{R(\delta, \mu)} \sin(I(\delta, \mu)), \end{aligned} \quad (6.29)$$

where we have applied the relations of equation (6.28) and it is defined

$$R(\delta, \mu) \equiv Re(i\delta^{3/2}w_{c,1}) \quad \text{and} \quad I(\delta, \mu) \equiv Im(i\delta^{3/2}w_{c,1}). \quad (6.30)$$

Therefore, the asymptotic transition probability is

$$\tilde{P} = 4 \left(\frac{\pi}{3}\right)^2 e^{2R(\delta, \mu)} \sin^2(I(\delta, \mu)). \quad (6.31)$$

The integrals of the form  $w_{c,1}$  appearing in the previous formulas are of the same form as those in the equation (4.72) and Shimshoni and Gefen also refer to the reference [32] and use similar change of variables. They also modify the result of

the integration one step further using the equation (15.4.14) of the reference [22] to obtain

$$\begin{aligned}
w_{c,1} &= \int_0^{\sqrt{i+\mu}} dy \sqrt{1 + (\mu - y^2)^2} \\
&= \frac{\pi e^{i\pi/4} (1 - i\mu) \sqrt{1 + i\mu}}{4} {}_2F_1 \left( -1/2, 1/2; 2; \frac{i + \mu}{-i + \mu} \right) \\
&= \frac{(i\pi)^{3/2} (1 + \mu^2)}{4} \left[ \frac{{}_2F_1(1/4, 5/4; 1/2; -\mu^2)}{\Gamma(\frac{3}{4}) \Gamma(\frac{7}{4})} - 2i\mu \frac{{}_2F_1(3/4, 7/4; 3/2; -\mu^2)}{\Gamma(\frac{5}{4}) \Gamma(\frac{1}{4})} \right].
\end{aligned} \tag{6.32}$$

It should be noted that the second line form of the equation (6.32) is almost the same as the equation (4.74), the latter differing from the first one by a factor of  $\delta^{3/2} = \sqrt{4/\epsilon}$ . However, from the definitions in equation (6.30) and the result of equation (4.74) we have the relations

$$R(\delta, \mu) = -\delta^{2/3} Im\Delta_c, \quad I(\delta, \mu) = \delta^{2/3} Re\Delta_c, \tag{6.33}$$

and the asymptotic transition probability in this notation is

$$\tilde{P} = 4 \left( \frac{\pi}{3} \right)^2 e^{-2Im\Delta_c} \sin^2(Re\Delta_c), \tag{6.34}$$

so that, actually, the result of Shimshoni and Gefen in the adiabatic limit also differs only by the prefactor  $\pi/3$  from the one obtained by the DDP method so that all the transition probabilities in it are larger by factor  $(\pi/3)^2 \approx 1.097$ .

We can conclude that there is no essential difference between the DDP results and those of Shimshoni and Gefen which is a fact that was not all that clear beforehand. Moreover, as our perturbation result coincided with the sudden limit result of Shimshoni and Gefen it is clear that their results do not really give us any significantly new contribution apart from the different phase factors for the independent crossing approximation and the alternative derivation of our results.



## 7 Comparison between different methods

The validity of different approximations were shortly discussed when introducing the different approximative methods in section 4. To gain a more complete view, we discuss them here in detail while comparing the results with those obtained by numerical simulations. The numerical calculations were done in a wide range of parameters so that one could be able to deduce the general behaviour of the system, at least qualitatively.

The most interesting cases are the double crossing ones, that is, the cases where  $\mu$  is positive. There one can see a diverse behaviour due to the interference effects. These are discussed in the first subsection and we represent the results for the parameters  $\mu = 0.1$ ,  $\mu = 1$ ,  $\mu = 3$  and  $\mu = 5$  when  $\epsilon$  is varied from 0 to 100. In the following subsections we also study similarly the tunneling cases with  $\mu = -0.1$  and  $\mu = -1$ , the limiting case of a single crossing with  $\mu = 0$  and also cases where the parameter  $\epsilon$  is fixed and  $\mu$  varies. These are all plotted in the figures 7 – 11. In the cases where  $\mu$  is fixed the  $\epsilon$ -axis is logarithmic because the general behaviour is that the transition probabilities are changing more rapidly with respect to  $\epsilon$  when  $\epsilon$  is sufficiently small. With larger values the population does not depend so sensitively on  $\epsilon$ . In the last subsection we discuss the different phases obtained for the independent crossing approximation to decide whether one of them is in a better correspondence with numerical results than the others.

### 7.1 The double crossing case

In the figure 7 we have the numerical result and different approximations for  $\mu = 0.1$  and  $\mu = 1$ . When  $\mu = 0.1$ , we have only one wide peak and the behaviour is still rather similar to single crossing or tunneling cases. It is also evident that none of the approximative curves gives right kind of results for all the values of  $\epsilon$ . However, one can see that the DDP curve is of the right shape and it does give right values

along with the modified DDP result in the adiabatic region which in this case means the values  $\epsilon < 1$ . For intermediate values of  $\epsilon$  there is no good approximation. The perturbation result is seen to give a good approximation for larger values of the variable. This is of course what the used scaling  $\epsilon \equiv a/v^3$  suggests: small coupling of the diabatic energy levels correspond to large values of  $\epsilon$  if we fix the parameter  $a$  and the same result holds for the other values of  $\mu$  as well.

For  $\mu = 1$  there is already some oscillations present and also a complete population transfer can be obtained. Here the DDP curve is again of the right shape but it diverges from the numerical result earlier than in the previous case giving values larger than unity. However, here the modified DDP result overlaps completely with the numerical result for values approximately from zero to five. For larger values it starts to diverge from the numerical result. Also, the independent crossing approximation meets with the modified DDP result from the value  $\epsilon = 1$  on, thus giving a good approximation for intermediate values.

The validity of the independent crossing approximation for these particular cases can be further studied from the equations (4.2) which give the time scale for a single Landau-Zener transition  $\tau_z$ . The approximation was expected to work whenever we have  $\tau_z \ll \tau_s$  where  $\tau_s$  is the time between the crossings. From this we derived the test for the validity in the section 4.1 which, when simplified, reads: in the adiabatic limit we have  $\Lambda_{\text{eff}} \gg 1$  and the condition is  $\mu \ll 1$  and in the diabatic limit ( $\Lambda_{\text{eff}} \ll 1$ ) the condition is  $(\mu^3/\epsilon) \gg 1/100$ . However, as  $\epsilon$  increases we move from adiabatic into diabatic region and we have to change the expression for  $\tau_z$  correspondingly, as suggested by the equation (4.2). It follows that in between them we have a parameter region where we have  $\Lambda_{\text{eff}} \approx 1$  and we do not have a test for the validity of the approximation. For example, when  $\mu = 1$  we see that in the region where  $\epsilon \in [0.1, 1]$  the independent crossing curve almost gives the right kind of behaviour but with too small values. It is in this parameter region the parameter

$\Lambda_{\text{eff}}$  decreases from the value  $\sqrt{5/2}$  to the value  $1/2$  and we do not have a clear time scale for the transitions or at least it is not given by the condition (4.2). From that point on, however, the curve overlaps with the numerical result until about the point  $\epsilon = 5$  onwards it again starts to diverge slightly. The reason for diverging is that the crossings start to slowly overlap already. At that point we still have  $(\mu^3/\epsilon) = 1/5$  which is relatively large when compared to the validity condition but also decreasing steadily as  $\epsilon$  increases.

The general trend is that as  $\mu$  has greater values the adiabatic test fails but at the same time both the time between the crossings and the region where the diabatic condition can be used and is valid becomes larger. For example, when  $\mu$  is multiplied by two,  $\epsilon$  can have eight times larger values before the approximation becomes invalid.

From the figure 8 one can also see that when  $\mu$  gets larger the plots get more rapidly oscillating and the value of the population becomes more sensitive to changes of  $\epsilon$ . Moreover, it is seen that the adiabatic region gets smaller and smaller with greater  $\mu$  and the DDP result diverges from the numerical one from early on giving unphysical values greater than unity. The perturbation method on the other hand becomes useful slightly earlier, compared to previous cases and this is of course what was expected from the scaling  $\mu \equiv b/v$ . However, the most noteworthy thing is that the modified DDP result and the double Landau-Zener result overlap completely in the studied parameter region of  $\epsilon$  when we have  $\mu = 3$  or  $\mu = 5$ . In the figures 10 and 11 where  $\epsilon$  is kept constant in each plot, it is seen that these two approximations seem to work really nicely with also larger positive values of  $\mu$  because of the overlap with the numerical results also in those cases.

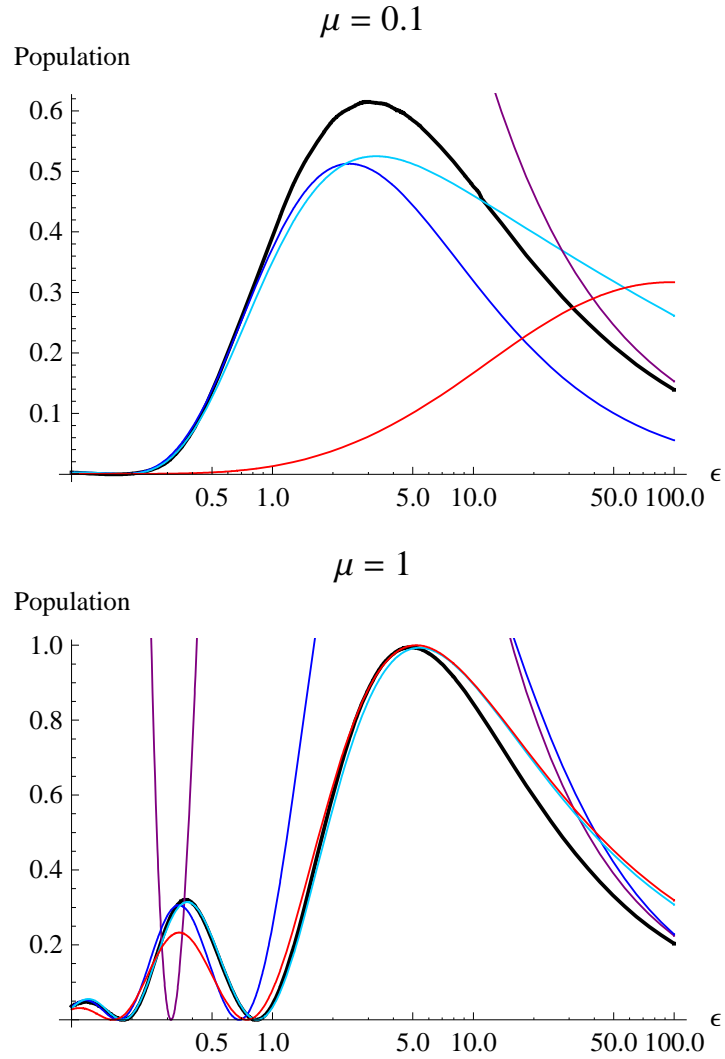


Figure 7. Here are the final populations  $P_1$  as functions of  $\epsilon$  for the cases  $\mu = 0.1$  and  $\mu = 1$  from top to bottom, respectively. The numerical result is represented by the black line, whereas the perturbation result is drawn as a purple line and the independent crossing approximation as a red line. The pure and modified DDP results are represented by dark blue and light blue lines, respectively.

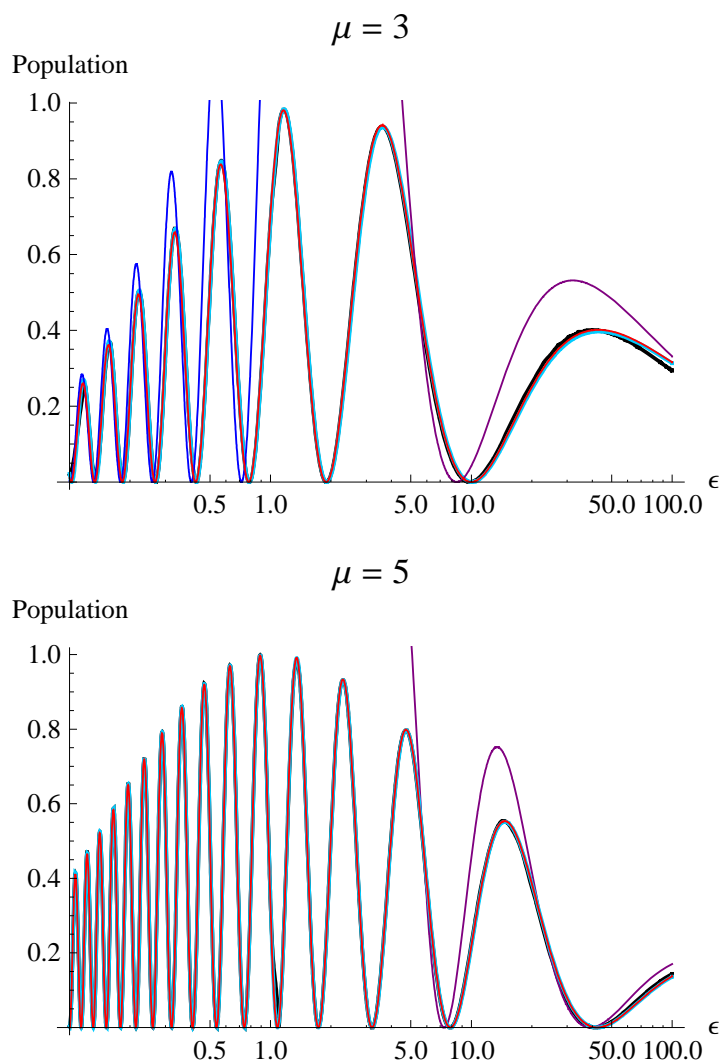


Figure 8. This figure is similar to Fig. 7 and with the same notation but for the cases  $\mu = 3$  and  $\mu = 5$  from top to bottom, respectively. For the case  $\mu = 3$  we have plotted the DDP result only up to the argument value  $\epsilon = 1$  as it diverges from the numerical result. Also, the perturbation result is plotted only from the value  $\epsilon = 5$  on as it does not give sensible results earlier. For the case  $\mu = 5$  we have omitted the DDP result altogether as it differs from the numerical result even earlier on.

## 7.2 The tunneling case

The single crossing and the two tunneling cases studied are plotted in the figure 9. The plots look all alike and are also similar to the case  $\mu = 0.1$ . It is also seen that the maximum transition probability decreases rapidly as  $\mu$  decreases, or equivalently, as the gap between the energy levels increases.

All of the approximations give a correct behaviour qualitatively but not correct values everywhere. The DDP method works in the adiabatic region and slightly better than the modified one. It should be noted that the phase term  $\chi$  is left out from the equation (4.78) for non-positive values of  $\mu$ . Also, the perturbation method works where it is expected to, namely for large  $\epsilon$ . However, none of the approximations cover the region with intermediate values of  $\epsilon$ .

## 7.3 The phases in the independent crossing approximation

The independent crossing approximation turned out to be a good and useful approximation in many cases, especially with sufficiently large positive values of the parameter  $\mu$ . From the discussion of the results of Shimshoni and Gefen we saw that their way of deriving the same approximation gave different phase terms than the one we obtained in the section 4.1 but that the enveloping curve was the same for both, given by the function  $e(\epsilon, \mu) \equiv 4e^{-\pi\Lambda_{\text{eff}}} (1 - e^{-\pi\Lambda_{\text{eff}}})$ . Because of the rapid oscillations, the results are sensitive to the phases so it is important to compare these results and to see if the results of Shimshoni and Gefen work in some regions better than our result.

In some ways this seems unlikely. First of all, the linearisation condition to ensure the validity of the approximation is of course the same for their result. Secondly, our result which consisted of a single formula for all the parameter regions worked very well for the parameters  $\mu > 1$ . Rather than just one expression, Shimshoni and Gefen derived different expressions for the adiabatic and diabatic limits and this too

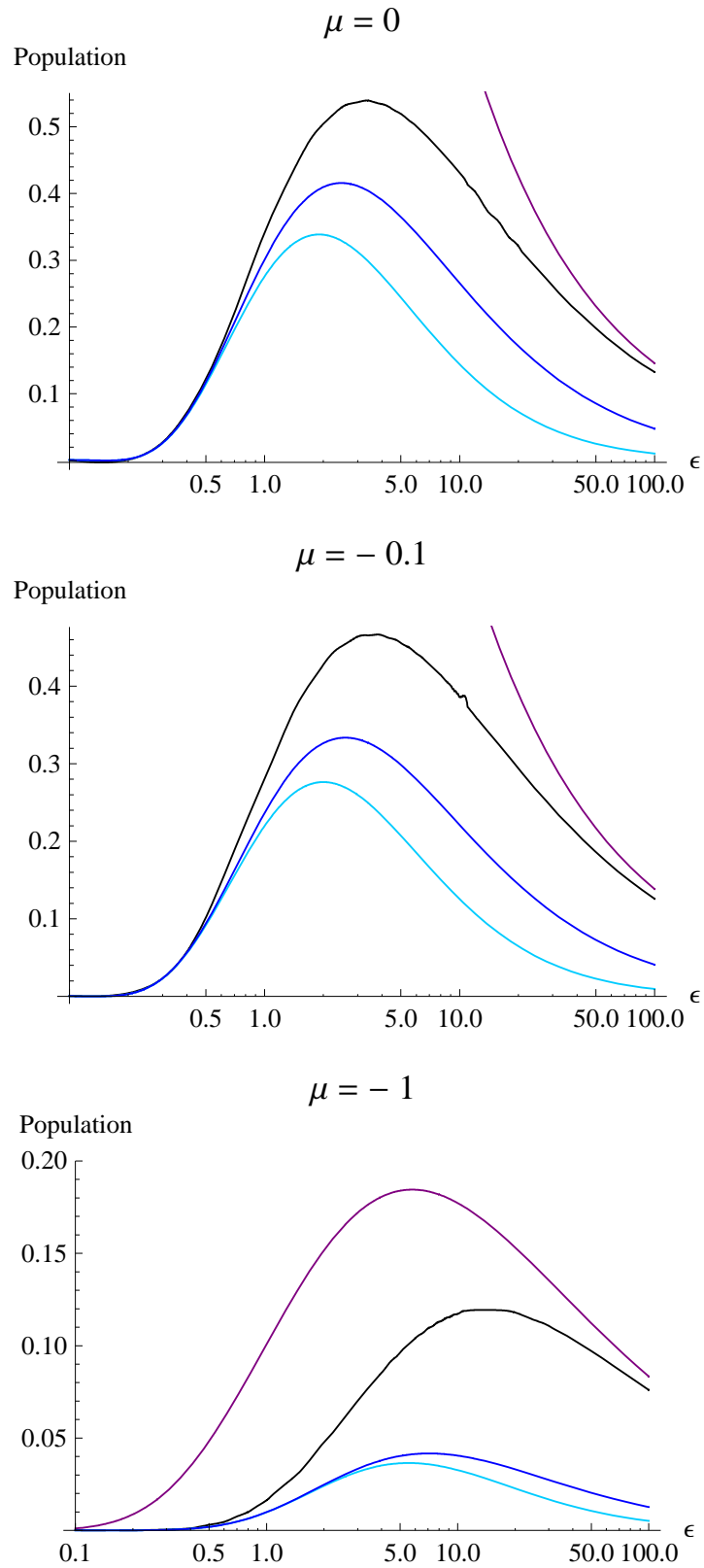


Figure 9. This figure is similar to the two previous ones and it covers the cases  $\mu = 0$ ,  $\mu = -0.1$  and  $\mu = -1$  from top to bottom, respectively. These are double crossing cases no more and therefore there are no oscillations visible. Also the Landau-Zener approximation is omitted as well as the  $\chi$  term in the modified DDP method.

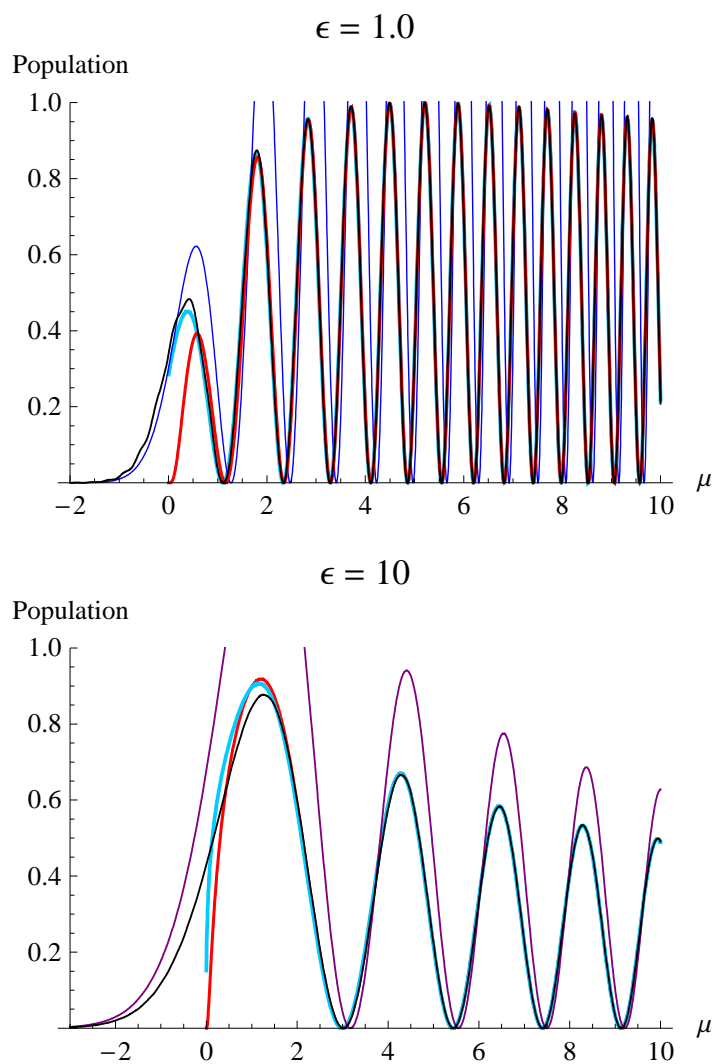


Figure 10. Here are the final populations  $P_1$  as a function of  $\mu$  and with fixed  $\epsilon$ . The color coding for the lines is the same as in the preceding figures but for the case  $\epsilon = 1$  the perturbation result is omitted because it would require higher values of  $\mu$  to be useful. For the case  $\epsilon = 10$ , the DDP plot is instead dropped because it diverges from the numerical result quite early on. The double Landau-Zener result and the modified DDP result are defined only for positive  $\mu$  but it is seen that from approximately  $\mu = 1$  on they overlap with the numerical result.



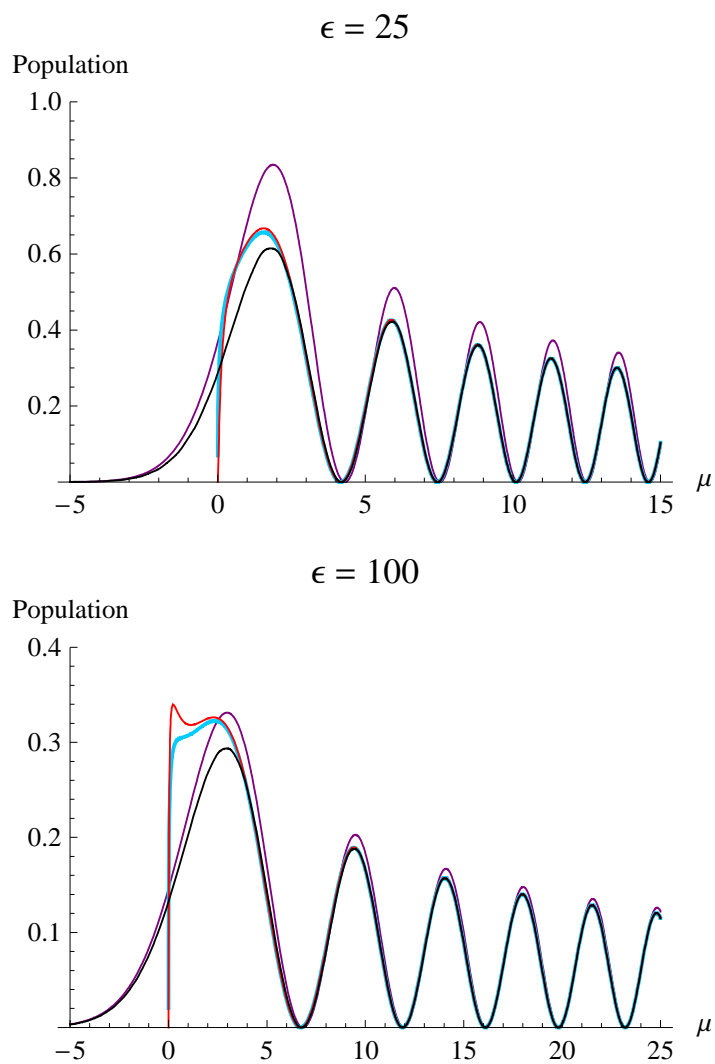


Figure 11. This is exactly similar to figure 10 but this time for the parameter values  $\epsilon = 25$  and  $\epsilon = 100$ , respectively from top to bottom. The DDP result is again omitted. The independent crossing result and the modified DDP result overlap again the numerical plot in a large part of the parameter range of  $\mu$ . This time also the perturbation method gives a rather good approximation already with quite small values of  $\mu$  as expected.

can be thought as a downside because then one has to also consider their different regions of validity and it is likely that neither of them is a good approximation for intermediate values, that is, between the adiabatic and diabatic limits. In any case, it is interesting to see if the results of Shimshoni and Gefen work as well as ours in general or even better with small values of  $\mu$ .

The different independent crossing results are plotted in the figures 12 and 13. One can immediately see that, indeed, our result seems to work much better. The results of Shimshoni and Gefen do work where they should, namely in the adiabatic and diabatic limits, but for the most part of the parameter range they both go wrong. Although, in the case for which  $\mu = 0.1$  all of the different independent crossing results break down, it is interesting how far off the adiabatic result of Shimshoni and Gefen goes from the correct numerical result. It does give correct values for small  $\epsilon$ , but then again, all of the double Landau-Zener results do because the modulation of the enveloping curve cuts them off. With larger values of  $\epsilon$  it remains barely visible above the  $\epsilon$ -axis.

Some insight to this and to the general behaviour of the results in this approximation can be attained by studying the phases, that is, the arguments in the sine term in the independent crossing result and same time taking to account the behaviour of the modulation of the envelope curve. We have plotted these phases in the figures 14 and 15. For the adiabatic result of Shimshoni and Gefen the phase consists only of the dynamical phase accumulated by the diabatic energy level as given by the equation (3.7). This phase term is small when either  $\mu$  is small or  $\epsilon$  is large. The diabatic result on the other hand, differs from it only by a constant factor of  $\pi/4$ .

It is readily seen that all of the different phases behave similarly by decreasing quite rapidly with increasing  $\epsilon$  and fixed  $\mu$ . The general behaviour is that as we increase the value of  $\mu$ , the phases get larger values and that the relative differences

between them get smaller. Also, the diabatic phase of Shimshoni and Gefen tends to our result in the diabatic region which is not surprising but the adiabatic phase does not in general do the same in the adiabatic region.

Of course, the absolute value of the phases is not really the essential quantity here. Because the sine squared has a periodicity of  $\pi$  we are more interested in the remainder when the values of the phases are divided by  $\pi$ . However, the absolute value of the phase does tell us something about the number of periods of oscillation in the parameter region. Another important quantity is the rate of the change of the phase as a function of  $\epsilon$  which is related to the periods of these oscillations. As the absolute values of the phase functions get larger along with the parameter  $\mu$  but still decrease to values near zero we see that the range of the values the phase gets is a higher multiple of  $\pi$  and therefore the number of periods of oscillations is larger. Similarly, when the phases decrease rapidly the period of these oscillations is small and as mentioned above, the rapid decrease of the phases happen with small  $\epsilon$ . On the other hand, we can also see that there still is no oscillations when  $\mu$  is sufficiently small. The reason for this is that the enveloping curve suppresses them as the maximum of the enveloping curve is given by the equation  $\epsilon_{\max} = \frac{1}{\mu} \left( \frac{\pi}{2 \ln 2} \right)^2$ . As  $\mu$  increases the maximum value is obtained with smaller  $\epsilon$  and the oscillations become visible.

From the figures 12 - 15, for example, we see that although the different phases behave similarly and are relatively close to each other the values of the different transition probabilities at some given point may differ largely due to rapid oscillations. It is therefore evident that the correct way to calculate the phases in the parabolic model is crucially important.

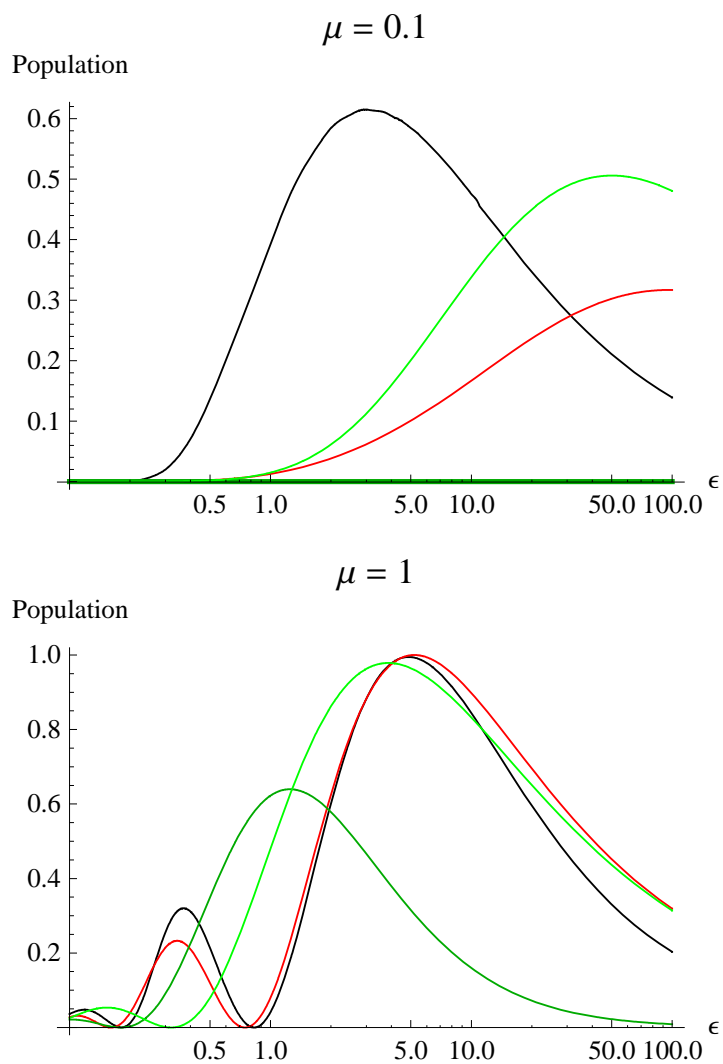


Figure 12. A comparison between the different independent crossing results which differ from each other only by the phase terms in the sine function. The populations are plotted here for the cases  $\mu = 0.1$  and  $\mu = 1$ , from top to bottom. Our result is again represented by the red line, the black line being again the numerical result. The adiabatic and diabatic expressions for the double Landau-Zener result of Shimshoni and Gefen and are plotted as a dark and light green lines, respectively.

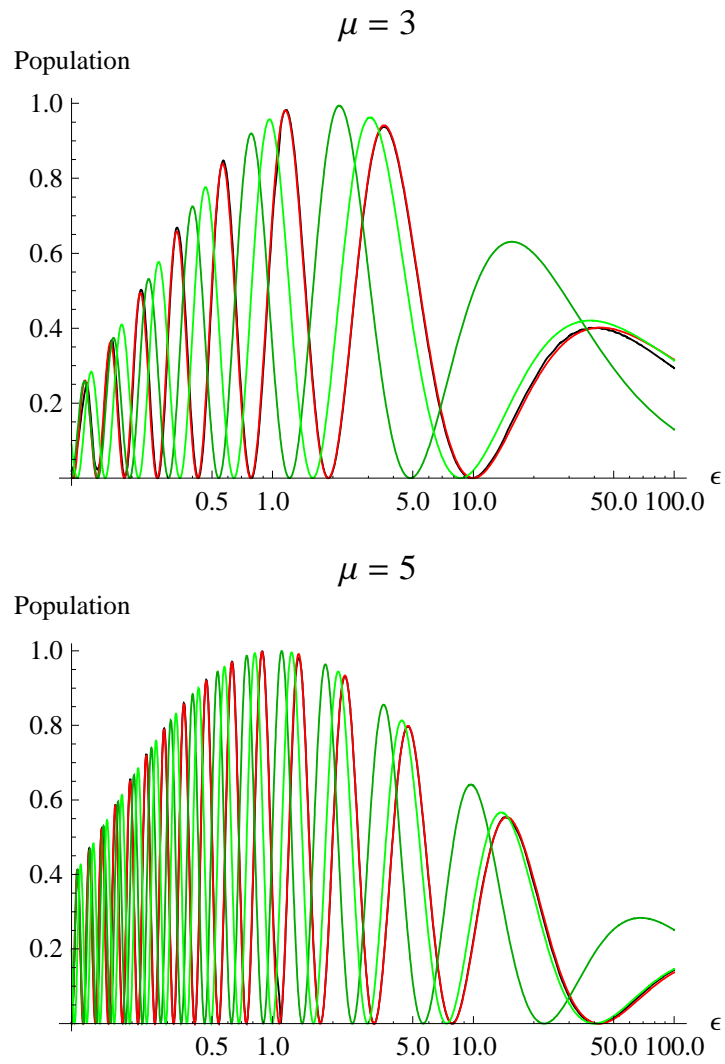


Figure 13. This is similar to the previous figure but here are the cases for  $\mu = 3$  and  $\mu = 5$ .

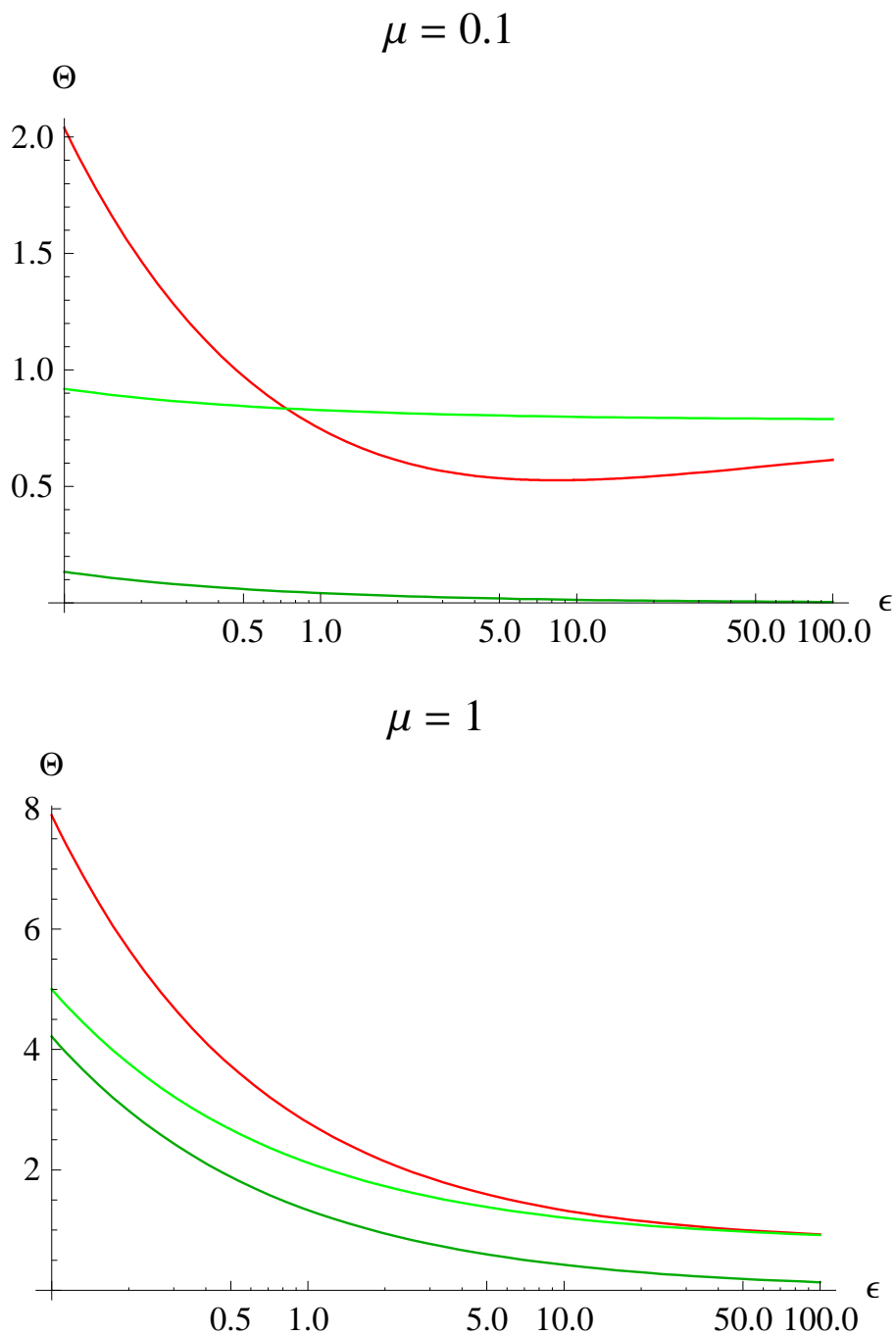


Figure 14. In this figure we have plotted the arguments  $\Theta$  of the sine term in the different independent crossing approximations as a function of  $\epsilon$  for the cases  $\mu = 0.1$  and  $\mu = 1$ . That is, the red line represents the overall phase term again for the double Landau-Zener result obtained in the section 4.1 while the light and dark green are respectively the corresponding sudden and adiabatic results of Gefen and Shimshoni.

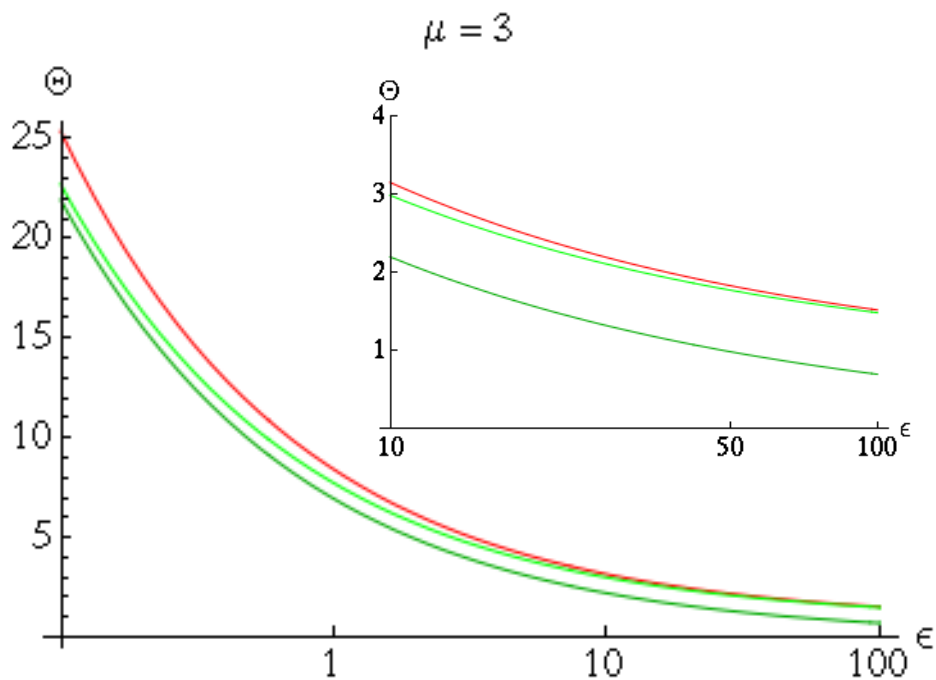


Figure 15. This figure is similar to previous one but containing the case  $\mu = 3$ . An inset has been added in order to make the behaviours of the different phases for large values of the parameter  $\epsilon$  more clear.

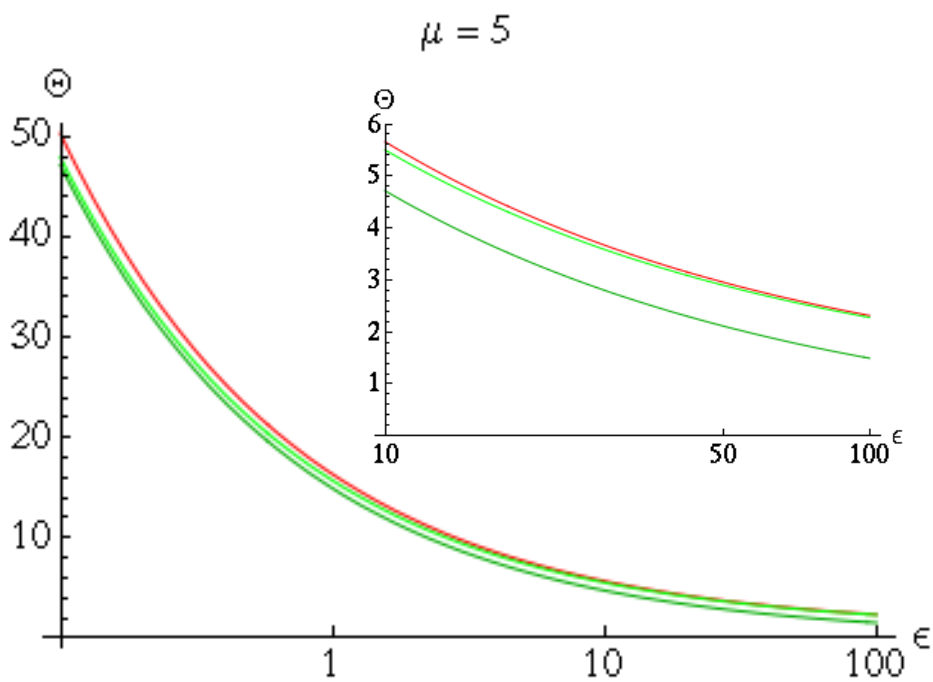


Figure 16. This figure is similar to previous one but it contains the case  $\mu = 5$ .

## 8 Conclusions

In this thesis we have studied simple level crossing models and some of the related phenomena in the two-level approximation. It was seen that even such simple systems could contain quite diverse behaviour and that solving the time evolution of the system is in general difficult. It was also seen that already the most simple of the level crossing models, the Landau-Zener model, was able to give some essential behaviour of the more complex systems. The emphasis, however, was on the dynamics of the parabolic level crossing model.

We considered many different approximative methods to obtain the asymptotic transition probabilities. In particular, the DDP method was discussed in depth and its derivation was performed in detail although perhaps other approximation methods turned out to be more useful in terms of simplicity and larger parameter region of applicability. The importance of the DDP method, however, is its rigorous mathematical basis and the fact that quite often the physical systems under study do behave nearly adiabatically and in those cases the numerical methods also get more time-consuming, therefore emphasising the need for analytical methods.

By slightly modifying the DDP method one could get an approximation that works beyond the adiabatic limit, although the derivation of the modified DDP method was largely of heuristic nature. However, it works nicely over the validity region of the double Landau-Zener result and contains also parameter regions where the assumption of independent crossings fails. In the tunneling cases the DDP method was found to give better results although in general the approximative method were less succesful than in the double crossing regions. We can conclude that the modified DDP method gives surprisingly good results but it would be important to have a more rigorous and firm derivation for it.

In this study we also recalculated and confirmed many of the results obtained in the reference [28], including the numerical results as well as some others. We also



compared these results to the results in the reference [41] which is something that has not been previously done. We found that there were a lot of similarities between the approach used in [41] and for example the DDP method but overall our results seemed to be in a better agreement with the numerical calculations. In particular, our expression for the phases in the independent approximation gave considerably better results. In any case, the double crossing character of the parabolic model highlighted the importance of the correct calculation of the phases.

## References

- [1] C. Zener, *Non-adiabatic crossing of energy levels*, Proc. R. Soc. London, A **137**, 696 (1932).
- [2] L. D. Landau, *Zur Theorie der Energieübertragung II*, Phys. Z. Sowjet Union **2**, 46 (1932), reprinted in English in D. ter Haar, *Collected Papers of L. D. Landau*, (Gordon and Breach, New York, 1967).
- [3] E. C. G. Stückelberg, Helv. Phys. Acta **5**, 370 (1932).
- [4] R. Requist, J. Schliemann, A. G. Abanov and D. Loss, *Double occupancy errors in quantum computing operations: corrections to adiabaticity*, arXiv:cond-mat/0409096v1 (2004).
- [5] B. M. Garraway and K.-A. Suominen, *Wave packet dynamics in molecules*, Contemp. Phys. **43**, 97 (2002).
- [6] R. N. Mohapatra and P. B. Pal, *Massive Neutrinos in Physics and Astrophysics*, (World Scientific, Singapore, 1991).
- [7] P. W. Anderson, *Concepts in solids*, (W. A. Benjamin Inc., Reading, 1963).
- [8] M. Sillanpää, T. Lehtinen, A. Paila, Y. Makhlin and P. Hakonen, *Continuous-time monitoring of Landau-Zener interference in a Cooper-pair box*, Phys. Rev. Lett. **96**, 187002 (2006).
- [9] A. P. Kazantsev, G. I. Surdutovich and V. P. Yakovlev, *Mechanical Action of Light on Atoms*, (World Scientific, Singapore, 1990).
- [10] S. Stenholm and K.-A. Suominen, *Quantum approach to informatics*, (John Wiley and Sons, Hoboken, 2005).
- [11] E. Prugovečki, *Quantum Mechanics in Hilbert Space, 2nd ed.*, (Academic Press, New York, 1981).
- [12] E. T. Whittaker and G. N. Watson, *A Course of Modern Analysis, 4th ed.*, (Cambridge University Press, Cambridge, 1927).
- [13] A. M. Dykhne, *Quantum transitions in the adiabatic approximation*, Sov. Phys. JETP **11**, 411 (1960).
- [14] A. M. Dykhne, *Adiabatic perturbation of discrete spectrum states*, Sov. Phys. JETP **14**, 941 (1962).
- [15] J. P. Davis and P. Pechukas, *Nonadiabatic transitions induced by a time-dependent Hamiltonian in the semiclassical/adiabatic limit: The two-state case*, J. Chem. Phys. **64**, 3129 (1976).
- [16] M. Born and V. Fock, *Beweis des Adiabatsatzes*, Z. Phys. A **51**, 165 (1928).

- [17] T. Kato, *On the Adiabatic Theorem of Quantum Mechanics*, J. Phys. Soc. Jap. **5**, 435 (1958).
- [18] J. E. Avron and A. Elgart, *Adiabatic theorem without a gap condition*, Commun. Math. Phys. **203**, 445 (1999).
- [19] A. Messiah, *Quantum Mechanics, Volume II*, (North-Holland, Amsterdam, 1962).
- [20] D. Chruściński and A. Jamiolowski, *Geometric phases in classical and quantum mechanics*, (Birkhäuser, Boston, 2004).
- [21] V. L. Pokrovsky and N. A. Sinitsyn, *On the generalized Landau-Zener problem*, arXiv:cond-mat/0012303v1 (2000).
- [22] M. Abramowitz and I. A. Stegun, *Handbook of Mathematical Functions*, (Dover, New York, 1970).
- [23] I. S. Gradshteyn and I. M. Ryzhik, *Table of Integrals, Series, and Products*, (Academic Press, New York, 1980).
- [24] C. M. Bender and S. A. Orszag, *Advanced Mathematical Methods for Scientists and Engineers*, (McGraw-Hill, New York, 1978).
- [25] K.-A. Suominen, *The Landau-Zener linear crossing problem and non-adiabatic transitions*, Report series in theoretical physics, University of Helsinki, (1990).
- [26] E. E. Nikitin, *Nonadiabatic transitions near the turning point in atomic collisions*, Opt. Spectrosc. USSR **11**, 246 (1961).
- [27] K.-A. Suominen, *Time dependent two-state models and wave packet dynamics*, Academic dissertation, Report series in theoretical physics, University of Helsinki, (1992).
- [28] K.-A. Suominen, *Parabolic level crossing models*, Optics Comm. **93**, 126 (1992).
- [29] B. M. Garraway and S. Stenholm, *Interferometer within a molecule*, Phys. Rev. A **46**, 1413 (1992).
- [30] R. Vasile, H. Mäkelä and K.-A. Suominen, *Interferometry using spinor Bose-Einstein condensates*, arXiv:quant-ph/0812.0499v1 (2008).
- [31] V. K. Bykhovskii, E. E. Nikitin and M. Y. Ovchinnikova, *Probability of a non-adiabatic transition near the turning point*, Sov. Phys. JETP **20**, 500 (1965).
- [32] D. S. F. Crothers and J. G. Hughes, *Stueckelberg close-curve-crossing phases*, J. Phys. B **10**, L557 (1977).
- [33] M. S. Child, *Molecular Collision Theory*, (Academic Press, London, 1974).

- [34] K. Mullen, E. Ben-Jacob, Y. Gefen and Z. Schuss, *Time of Zener Tunneling*, Phys. Rev. Lett. **62**, 2543 (1989).
- [35] J. Paldus, *Perturbation Theory*, in Drake, G. W. F. (Ed.) *Springer Handbook of Molecular, Atomic and Optical Physics*, (Springer, New York, 2006).
- [36] A. Shapere and F. Wilczek, *Geometric Phases in Physics*, (World Scientific, Singapore, 1989).
- [37] J.-T. Hwang and P. Pechukas, *The adiabatic theorem in the complex plane and the semiclassical calculation of nonadiabatic transition amplitudes*, J. Chem. Phys. **67**, 4640 (1977).
- [38] M. V. Berry, *The adiabatic limit and the semiclassical limit*, J. Phys. A **17**, 1225 (1984).
- [39] Wolfram Research, Inc., Mathematica, Version 6.0, Champaign, IL (2007).
- [40] Private discussions with professor K.-A. Suominen at the University of Turku during Summer 2009.
- [41] E. Shimshoni and Y. Gefen, *Onset of dissipation in Zener dynamics: relaxation versus dephasing*, Ann. Phys. **210**, 16 (1991).
- [42] M. V. Berry, *Histories of adiabatic quantum transitions*, Proc. R. Soc. London A **429**, 61 (1990).